



저작자표시-비영리-변경금지 2.0 대한민국

이용자는 아래의 조건을 따르는 경우에 한하여 자유롭게

- 이 저작물을 복제, 배포, 전송, 전시, 공연 및 방송할 수 있습니다.

다음과 같은 조건을 따라야 합니다:



저작자표시. 귀하는 원저작자를 표시하여야 합니다.



비영리. 귀하는 이 저작물을 영리 목적으로 이용할 수 없습니다.



변경금지. 귀하는 이 저작물을 개작, 변형 또는 가공할 수 없습니다.

- 귀하는, 이 저작물의 재이용이나 배포의 경우, 이 저작물에 적용된 이용허락조건을 명확하게 나타내어야 합니다.
- 저작권자로부터 별도의 허가를 받으면 이러한 조건들은 적용되지 않습니다.

저작권법에 따른 이용자의 권리는 위의 내용에 의하여 영향을 받지 않습니다.

이것은 [이용허락규약\(Legal Code\)](#)을 이해하기 쉽게 요약한 것입니다.

[Disclaimer](#)

이학석사 학위논문

**Behaviors of REEs and Trace Metals
in the Nakdong River Estuary,
Obstructed by a Dam**

댐이 있는 낙동강 하구에서의
희토류와 미량 금속의 거동

2021 년 2 월

서울대학교 대학원

지구환경과학부

김 예 립

**Behaviors of REEs and Trace Metals
in the Nakdong River Estuary,
obstructed by a dam**

지도교수 김 규 범

이 논문을 이학석사 학위논문으로 제출함

2021 년 2 월

서울대학교 대학원

지구환경과학부

김 예 립

김예림의 이학석사 학위논문을 인준함

2021 년 2 월

위 원 장

황 점 식

 (인)

부위원장

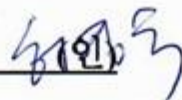
김 규 범

 (인)

위

원

허 영 숙

 (인)

Abstract

**Behaviors of REEs and Trace Metals
in the Nakdong River Estuary,
Obstructed by a Dam**

Yerim Kim

School of Earth and Environmental Sciences

The Graduate School

Seoul National University

Dams obstruct approximately 70% of the rivers across the world. However, their effect on the riverine fluxes of rare earth elements (REEs) and trace metals needs more research. In order to investigate the mixing process and evaluate the influence of a dam on the estuary, dissolved REEs and trace metals were examined throughout the whole season in the Nakdong River Estuary, Korea. Samples were concentrated beforehand using a preconcentration system (seaFAST), then analyzed by inductively coupled plasma mass spectrometry (HR-ICP-MS). The REEs showed a conservative mixing trend, but with systematic changes across the series due to varying river water endmember concentration. Fractionation of the REEs seems to take place. The shale-normalized REEs also supported this result, as they showed lower LREEs in the whole sampling period. Mn and Co increased with salinity but

showed exceptionally high and scattered concentrations in the low-salinity region ($S = 0-7$) in October and July, similar to the LREEs. The discharge of river water with various concentrations from the dam explains the scattered riverine endmember. The redox reaction of Mn appears to account for the inhomogeneous vertical water column of elements inside the dam. The scatter converged to the oceanic endmember in the higher salinity region ($S = 7-28$) as the discharged freshwater physically mixes with seawater. The redox reaction and mixing also seems to affect the distribution of Cd and Ni. Fe showed an abrupt decrease in the low-salinity region that may result from a drastic removal by flocculation throughout the whole sampling period. Mo and V showed a positive correlation with increasing salinity since they originate from the ocean. Cu and Gd decreased conservatively, staying stable by binding with dissolved organic carbon and chelate ligands. The fraction of Gd from anthropogenic and natural sources was estimated, and it suggested that anthropogenic Gd remains constant by forming chelate complexes after release. This study displays both chemical and physical processes in the estuary and suggests that reactions inside a dam may affect the riverine fluxes of REEs and trace metals.

Keywords: Estuary, rare earth elements, trace metals, river water-seawater mixing, dam

Student Number: 2019-23097

Table of Contents

Chapter 1. Introduction	1
1.1. Rare Earth Elements.....	1
1.2. Trace Metals	2
1.3. Behaviors of Rare Earth Elements and Trace Metals in Estuaries	3
1.4. Dam Hydrology.....	6
1.5. Aim of This Study	7
Chapter 2. Materials and Methods	12
2.1. Study Site	12
2.2. Analysis.....	13
2.2.1. Sample Collection	13
2.2.2. Preconcentration of Rare Earth Elements and Trace Metals.....	14
2.2.3. Instrumental Analysis.....	15
2.2.4. Data Collection and Quality Control.....	16
Chapter 3. Results.....	26
3.1. Rare Earth Elements.....	26
3.1.1. Distributions of Dissolved Rare Earth Elements.....	26
3.1.2. Shale-Normalized Pattern of Dissolved Rare Earth Elements	33
3.2. Trace Metals	37
Chapter 4. Discussion	42
4.1. Fractionation of the Dissolved Rare Earth Elements	42
4.2. Features Observed in Dissolved Rare Earth Elements and Trace Metals	45

4.2.1. Mn, Co, and LREEs	45
4.2.2. Cd and Ni	51
4.2.3. Fe.....	51
4.2.4. Mo, V, Cu, and Gd	52
4.3. The Anthropogenic Fraction of Gd	55
Chapter 5. Conclusion	59
Bibliography.....	61
국문 초록	71

List of Tables

[Table 1] Elemental fluxes to the World Ocean from the major sources. (Units: mol · yr ⁻¹) Modern Anthropogenic Inputs are excluded. Reproduced from (Chester, 2009).	11
[Table 2] Operating conditions for high resolution inductively coupled plasma mass spectrometry (HR-ICP-MS)	23
[Table 3] Measured values of rare earth elements and trace metals for certified reference materials (SLRS-4 and CASS-6). (a) (Yeghicheyan et al., 2001), n=174, (b) (Ma et al., 2019), n=2	24
[Table 4] Reagent blanks and instrument detection limits of rare earth elements (n=9) and trace metals (n=12)	25
[Table 5] Concentrations of rare earth elements against salinities. (N.D.: Not Detected).....	29
[Table 6] Concentrations of trace metals against salinities. (N.D.: Not Detected, Numbers highlighted in red are considered as outliers.).....	40
[Table 7] The sample collection date, discharge, and average discharge value of the Nakdong River Estuary. The value of discharge is measured from the left bank drainage gate in the Nakdong River, where the sampling station is located.....	50
[Table 8] Calculated values of monthly average natural and anthropogenic Gd concentrations and their proportions.	57

List of Figures

[Figure 1] Rare earth elements and trace metals in the periodic table. Modified from https://www.philipharris.co.uk/blog/secondary/international-year-of-the-periodic-table/	8
[Figure 2] Various reactions occurring in the estuarine environment. Modified from (Pavoni et al., 2020).	9
[Figure 3] Distributions of rare earth elements against salinities in various estuaries. Reproduced from (Sholkovitz and Szymczak, 2000).	10
[Figure 4] Schematic diagrams of the overall analytical procedure for rare earth elements and trace metals.	18
[Figure 5] Location of sampling station in the Nakdong River Estuary. Modified from (Lee and Kim, 2018).	19
[Figure 6] (a) Schematic overview of the seaFAST preconcentration column. Reproduced from Elemental Scientific. (b) Chemical structure of functional groups on Nobias Chelate-PA1. Reproduced from (Sohrin et al., 2008). .	20
[Figure 7] Schematic overview of the high resolution inductively coupled plasma mass spectrometry (HR-ICP-MS). Modified from (Jakubowski et al., 1998).	21
[Figure 8] Instruments used in this study: SeaFAST SP3 system (right) connected to high resolution inductively coupled plasma mass spectrometry (HR-ICP-MS) (left).	22
[Figure 9] Graphs of dissolved rare earth elements versus salinities in the	

Nakdong River Estuary.....	28
[Figure 10] The monthly average PAAS (Post-Archean average Australian Shale) normalized patterns of dissolved REEs in the Nakdong River Estuary. The gray line indicates data collected in November 2017 from the same station (Kim et al., 2020).	36
[Figure 11] Dissolved concentrations of trace metals (V, Mn, Fe, Co, Ni, Cu, Cd, and Mo) against salinities in the Nakdong River Estuary.....	39
[Figure 12] Graphs of dissolved La, Eu, Lu concentrations versus salinity in the Nakdong River Estuary. The trendline is made from the data collected in the Nakdong River Estuary, November 2017 (Kim et al., 2020).	44
[Figure 13] LREE/HREE ratio against salinities in the Nakdong River Estuary.	48
[Figure 14] Conceptual diagram of redox reaction of Mn-oxide and function of the dam with respect to varying river water endmember concentration.	49
[Figure 15] Dissolved Cu concentration against dissolved organic carbon and humic colored dissolved organic matter in the Nakdong River Estuary. ..	54
[Figure 16] Schematic diagram of calculating anthropogenic and natural fraction in dissolved Gd.....	56
[Figure 17] Calculated fractions of monthly average anthropogenic and natural Gd from the Nakdong River Estuary.	58

1. Introduction

1.1 Rare Earth Elements

Rare earth elements (REEs) are a series of elements that consist of 14 lanthanide elements from La to Lu (Figure 1). These elements show chemically similar behavior owing to their electron configuration. The elements mostly exist in a trivalent state, except Ce and Eu. The ionic radius of the REEs decreases from La to Lu due to the nuclear charge increase. This phenomenon is known as the lanthanide contraction, which leads to systematically varying chemical affinity of the elements. In an aquatic environment, the REEs generally exist in trivalent oxidation states, except for Ce^{4+} and Eu^{2+} . Ce^{4+} is less soluble than Ce^{3+} , resulting in less release than neighboring elements in an aqueous solution (Sholkovitz and Szymczak, 2000). Such anomalous behavior of dissolved Ce usually occurs in natural waters. Their mass often groups the REEs as light REE (LREE; La to Nd), middle REE (MREE; Sm to Ho), and heavy REE (HREE; Er to Lu). Dissolved LREEs are more reactive with particles than dissolved HREEs. The LREEs are likely to be removed by processes such as surface adsorption onto particles through binding with a surface layer of organic matter or Fe, Mn oxides, or coagulation with colloids (Goldberg et al., 1963; Sholkovitz et al., 1993; Zhang and Nozaki, 1996). HREEs stay conservative by forming complexes with organic ligands in an aquatic environment (Tang and Johannesson, 2007). The varying reactivity of the elements along the series induces fractionation. The fractionation of dissolved REEs can work as a good indicator for investigating geochemical processes such as complexation, ad/desorption, and water source determination (Klinkhammer et al., 1983; Taylor and McLennan, 1981; Johannesson et al., 1997).

REEs have been utilized for industrial uses, and as a result, elements exceeding their natural concentration flows to the aquatic environment. Enrichment in REE through anthropogenic activities such as magnetic resonance imaging (MRI), batteries, and cell phones has been observed in rivers, estuarine systems, and oceans (Bau and Dulski, 1996; Nozaki et al., 2000a; Elbaz-Poulichet et al., 2002; Bau et al., 2006; Ogata and Terakado, 2006; Kulaksız and Bau, 2011; Kulaksız and Bau, 2013; Hatje et al., 2016). Above all, Gd is now regarded as the most widespread and effective tracer for industrial activities. Gd complexes have been used as a contrast agent for MRI since the 1980s. Since Gd^{3+} ions can bind to Ca^{2+} -binding enzymes, it can be dangerous to patients when directly injected (Sherry et al., 2009; Rogosnitzky and Branch, 2016). In order to eliminate the risk, Gd has been used only after chelation with ligands for chemical inertness and high stability (Hatje et al., 2018). The chelation enables Gd to be removed from the body as urine within 24 hours with normal kidney function. After evacuation from the human body, the Gd chelate compound stays conservative with half-lives of more than 100 days in an aquatic environment (Holzbecker et al., 2005; Moeller et al., 2000; Knappe et al., 2005; Rogowska et al., 2018). Accordingly, the additional input of Gd results in positive Gd anomalies, and the anomalies are utilized to indicate anthropogenic pollutants (Kulaksız and Bau, 2007).

1.2 Trace Metals

Trace metals (or often called trace elements) are a group of elements mostly comprised of metals or metalloids occurring at trace levels in the aquatic environment (Figure 1). These elements are usually present at concentrations less than $10\ \mu\text{mol kg}^{-1}$ in seawater and typically below one ppm in river water (Gaillardet

et al., 2003; Bruland and Lohan, 2003; Libes, 2011). Despite their low concentration, trace metals play a significant role in biogeochemical cycles. Previous studies reported that Fe, Mn, and Zn are just as essential as macronutrients like phosphorus and nitrogen due to their role as constraints limiting the growth of marine biota. (Cooper, 1935; Harvey, 1960; Brand et al., 1983; Tagliabue et al., 2017). Elements such as Cd, Co, Ni, and Mo are also crucial for nitrogen and carbon fixation, significantly influencing marine biological production (Morel and Price, 2003; Bruland and Lohan, 2003). Dissolved trace metals in seawater originate from various sources, including rivers, atmosphere, submarine groundwater discharge, and hydrothermal vents. With respect to the riverine input, dissolved trace metals mainly derive from geological pathways, including geological weathering of crustal rocks, geothermal and volcanic activities, and submarine groundwater discharge. Also, a substantial amount of direct input by anthropogenic activities such as municipal waste, agriculture, mining, and industrial waste around the river catchment and coastal ocean affect the aquatic system (Gaillardet et al., 2003). Various reactions govern dissolved trace metals in the hydrosystem (e.g., redox reactions, complexation, adsorption, desorption, scavenging by particulate matter). Due to their low concentration and the high possibility of interference by major ions in samples, trace metals have faced several analytical problems in terms of measurement. To overcome these issues, ultra-clean sampling, and measurement techniques were introduced in trace metal analysis (Boyle and Edmond, 1975; Boyle et al., 1976; Bender et al., 1976; Boyle et al., 1977; Bruland et al., 1979; Libes, 2011).

1.3 Behaviors of Rare Earth Elements and Trace Metals in Estuaries

An estuary is an extensive term referring to a region where one or more rivers join

the sea. Physical, chemical, and biogeochemical reactions occur dynamically throughout this chemical continuum of crustal rocks, rivers, and the ocean (Elderfield et al., 1990). When the river reaches the coastal sea, the river releases a vast amount of trace metals and REEs into the seawater. During the discharge, multiple factors including pH, salinity, temperature, organic ligands, inorganic anions, suspended particulate matter (SPM), and dissolved O₂ rapidly changes by mixing of freshwater, sediment, and seawater, creating a unique aquatic environment for trace metals and REEs (Millward, 1995). The transition brings about various reactions such as particle/solution interactions, flocculation, organic and inorganic complexation, adsorption, desorption, and sediment resuspension (Figure 2). As serving its role as an intricate biogeochemical reactor, the estuarine environment needs more research in order to fully understand the behaviors of dissolved REEs and trace metals (Millward, 1995).

Dissolved REEs except for Ce exhibited similar behaviors in estuaries owing to their similar chemical properties. The anomaly of dissolved Ce shows comparatively low concentration with adjacent elements due to different preferable oxidation states. The general trends of dissolved REEs vary depending on salinity in estuaries, where multiple geochemical reactions contribute to their behaviors. In the low-salinity region (generally $S = 0-7$), REEs typically show a drastic decline, far below the conservative mixing line of river water endmembers and seawater endmembers. (Sholkovitz, 1993; Nozaki et al., 2000b). Large-scale removal of dissolved elements caused by flocculation and coagulation induced by high turbidity in estuaries explains the decrease (Sholkovitz, 1993; Sholkovitz and Szymczak, 2000) (Figure 3). After the abrupt decrease, the dissolved REEs show an increase with increasing salinity. Several mechanisms such as the release of elements bound to SPM from the low-salinity region and the remineralization that supplies REEs through sediment

diagenesis commonly contribute to such trends (Sholkovitz, 1993; Nozaki et al., 2000b; Sholkovitz and Szymczak, 2000) (Figure 3). When the estuary finally reaches the high-salinity region ($S = 20-25$) where seawater dominates the area, the dissolved REEs gradually approaches that of the average seawater value, following a conservative mixing line. Although dissolved REEs generally exhibit similar patterns due to their coherence, the fractionation of the REEs presents some noticeable differences. The pH conditions and surface/solution reaction mainly control the fractionation in the estuarine environment, which leads to the variation of removal (Sholkovitz, 1995). The removal of dissolved REEs by adsorption onto the surface of river particles occurs in an order $LREEs > MREEs > HREEs$ as the pH increases, and the release of elements happens in the same order as the pH decreases (Sholkovitz, 1995). Furthermore, the addition of seawater to river water in estuaries also causes the removal of dissolved REEs by coagulation with riverine colloids, which occurs in the same order with adsorption, which can be observed by LREE-enriched colloids (Elderfield et al., 1990; Sholkovitz, 1995). A thorough understanding of the fractionation behavior by mixing between river water and seawater may function as an essential tracer to figure out the biogeochemical processes in the estuarine environment.

Although they do not show similarity with each other as dissolved REEs do, the dissolved trace metals behave diversely since spatially, and temporally varying factors (i.e., pH, salinity, ligands) govern numerous reactions in estuaries. The riverine flux of trace metals, which is known to be the primary source, generally exists in particulate form (Libes, 2011) (Table 1). Accordingly, most of the flux settles down in estuaries, and only 10% enters the ocean (Libes, 2011) (Table 1). Mechanisms that contribute to the behavior of trace metals are diverse; the elements are removed by reactions such as precipitation, adsorption onto SPM or sediment,

and biological uptake, while complexation with dissolved organic ligands such as humic acids, chelation with inorganic anion, and chemical speciation can stabilize the trace metals so that they can stay in dissolved form in estuarine water (Boyle et al., 1977; Sholkovitz and Copland, 1981). Even though removal of more than half of the elements occurs while passing the estuary, fluvial fluxes of trace metals still manage to be the critical source for the ocean to keep the marine biogeochemical cycle. Therefore, comprehension of the estuarine environment is essential to identify the trend of trace metals.

1.4 Dam Hydrology

Estuary provides water for various municipal purposes around cities formed near rivers and coastal areas. Humans constructed dams to regulate rivers and streams for higher accessibility and to prevent inundation and saltwater intrusion. Currently, there are over 58,000 dams constructed around the world, and that is, over 60% of the world's estuaries and rivers are obstructed (ICOLD 2020). By intentionally blocking the natural flow, the dam produces a new hydrologic regime where its chemical and physical properties are no longer the same as natural flows. Unfortunately, the direct effect of dams on REEs and trace metals' behavior was yet profoundly discussed. Several studies focused on the spatial and temporal distribution of elements in rivers with dams. However, the influence of a dam was likely to be ignored or generally regarded as a barrier located at the head of an estuary, which enables the sole evaluation of the riverine input of trace metals by inhibiting other water sources (Breuer and Sañudo-Wilhelmy, 1999; Shiller, 2002; Zhao et al., 2012). Profound knowledge of dams' influence on the distribution of REEs and trace metals will help to assimilate the estuarine chemistry.

1.5 Aim of This Study

The main goal of this study is to enhance the current knowledge about the distribution of REEs and trace metals in an estuarine environment and the effect of dams on these elements by evaluating their monthly concentration in Nakdong River Estuary, Korea. The objectives of this study include (1) understanding the process which governs the behavior of REEs and trace metals in an estuarine environment, including anthropogenic factors, and (2) evaluating the role of a dam; whether it affects the geochemical condition which contributes to the distribution of elements..

1 IA	2 IIA											13 IIIA	14 IVA	15 VA	16 VIA	17 VIIA	18 VIIIA
1 H Hydrogen 1.008																	2 He Helium 4.002602
3 Li Lithium 6.94	4 Be Beryllium 9.0121831											5 B Boron 10.81	6 C Carbon 12.011	7 N Nitrogen 14.007	8 O Oxygen 15.999	9 F Fluorine 18.99840363	10 Ne Neon 20.1797
11 Na Sodium 22.98976928	12 Mg Magnesium 24.305											13 Al Aluminium 26.9815385	14 Si Silicon 28.085	15 P Phosphorus 30.973761998	16 S Sulfur 32.06	17 Cl Chlorine 35.45	18 Ar Argon 39.948
19 K Potassium 39.0983	20 Ca Calcium 40.078	21 Sc Scandium 44.955908	22 Ti Titanium 47.867	23 V Vanadium 50.9415	24 Cr Chromium 51.9961	25 Mn Manganese 54.938044	26 Fe Iron 55.845	27 Co Cobalt 58.933194	28 Ni Nickel 58.6934	29 Cu Copper 63.546	30 Zn Zinc 65.38	31 Ga Gallium 69.723	32 Ge Germanium 72.630	33 As Arsenic 74.921595	34 Se Selenium 78.971	35 Br Bromine 79.904	36 Kr Krypton 83.798
37 Rb Rubidium 85.4678	38 Sr Strontium 87.62	39 Y Yttrium 88.90584	40 Zr Zirconium 91.224	41 Nb Niobium 92.90637	42 Mo Molybdenum 95.95	43 Tc Technetium (98)	44 Ru Ruthenium 101.07	45 Rh Rhodium 102.90550	46 Pd Palladium 106.42	47 Ag Silver 107.8682	48 Cd Cadmium 112.414	49 In Indium 114.818	50 Sn Tin 118.710	51 Sb Antimony 121.760	52 Te Tellurium 127.60	53 I Iodine 126.90447	54 Xe Xenon 131.293
55 Cs Caesium 132.90545196	56 Ba Barium 137.327	57 - 71 Lanthanoids	72 Hf Hafnium 178.49	73 Ta Tantalum 180.94788	74 W Tungsten 183.84	75 Re Rhenium 186.207	76 Os Osmium 190.23	77 Ir Iridium 192.217	78 Pt Platinum 195.084	79 Au Gold 196.966569	80 Hg Mercury 200.592	81 Tl Thallium 204.38	82 Pb Lead 207.2	83 Bi Bismuth 208.98040	84 Po Polonium (209)	85 At Astatine (210)	86 Rn Radon (222)
87 Fr Francium (223)	88 Ra Radium (226)	89 - 103 Actinoids	104 Rf Rutherfordium (261)	105 Db Dubnium (268)	106 Sg Seaborgium (269)	107 Bh Bohrium (270)	108 Hs Hassium (269)	109 Mt Meitnerium (278)	110 Ds Darmstadtium (281)	111 Rg Roentgenium (282)	112 Cn Copernicium (285)	113 Nh Nihonium (286)	114 Fl Flerovium (289)	115 Mc Moscovium (289)	116 Lv Livermorium (293)	117 Ts Tennessine (294)	118 Og Oganesson (294)

57 La Lanthanum 138.90547	58 Ce Cerium 140.16	59 Pr Praseodymium 140.90766	60 Nd Neodymium 144.242	61 Pm Promethium (145)	62 Sm Samarium 150.36	63 Eu Europium 151.964	64 Gd Gadolinium 157.25	65 Tb Terbium 158.92535	66 Dy Dysprosium 162.500	67 Ho Holmium 164.93033	68 Er Erbium 167.259	69 Tm Thulium 168.93422	70 Yb Ytterbium 173.045	71 Lu Lutetium 174.9668
89 Ac Actinium (227)	90 Th Thorium 232.0377	91 Pa Protactinium 231.03588	92 U Uranium 238.02891	93 Np Neptunium (237)	94 Pu Plutonium (244)	95 Am Americium (243)	96 Cm Curium (247)	97 Bk Berkelium (247)	98 Cf Californium (251)	99 Es Einsteinium (252)	100 Fm Fermium (257)	101 Md Mendelevium (258)	102 No Nobelium (259)	103 Lr Lawrencium (260)

Figure 1. Rare earth elements and trace metals in the periodic table.

Modified from <https://www.philipharris.co.uk/blog/secondary/international-year-of-the-periodic-table/>.

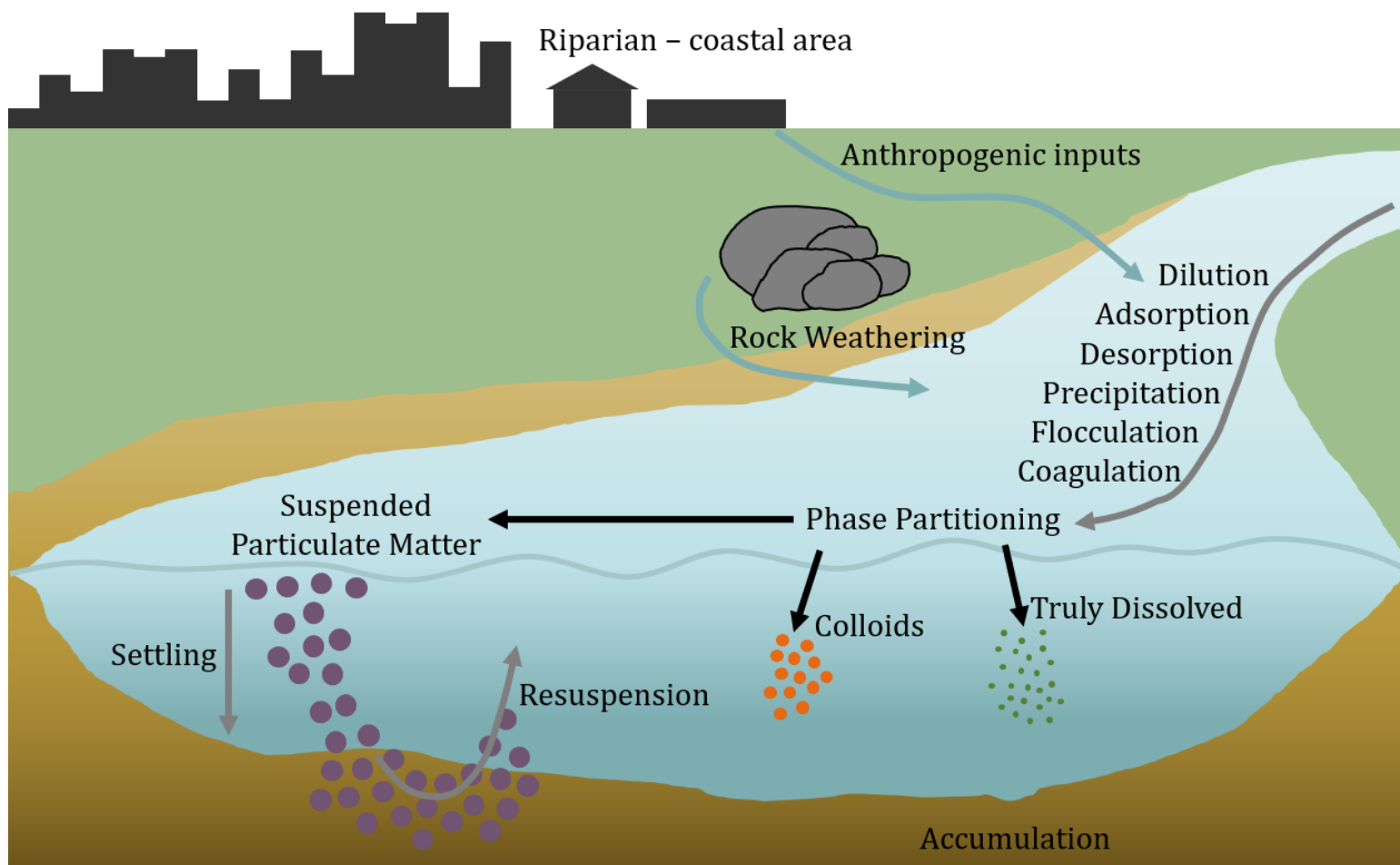


Figure 2. Various reactions occurring in the estuarine environment. Modified from (Pavoni et al., 2020).

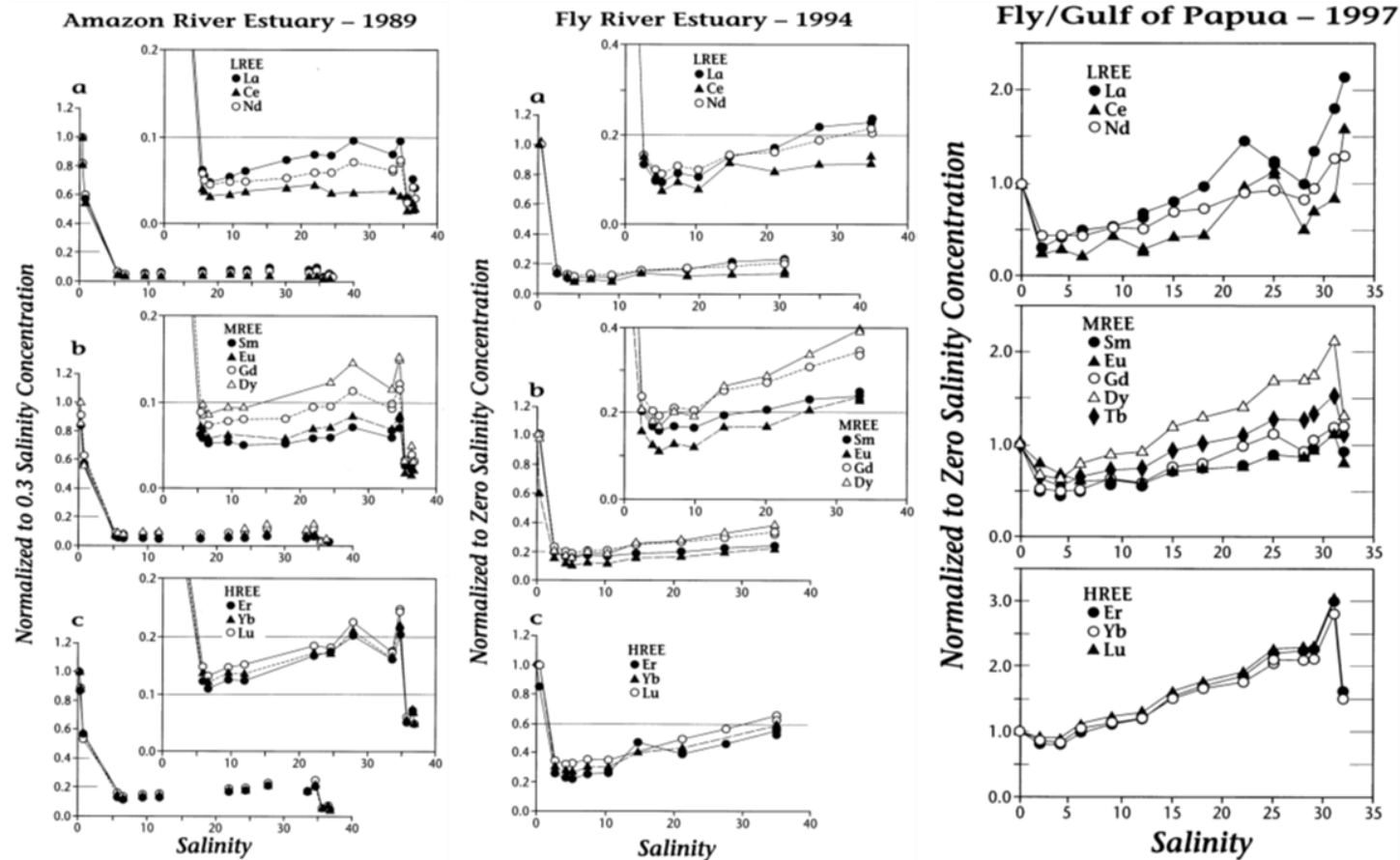


Figure 3. Distributions of rare earth elements against salinities in various estuaries. Reproduced from (Sholkovitz and Szymczak, 2000).

Table 1 Elemental fluxes to the World Ocean from the major sources. (Units: mol · yr⁻¹)

Modern Anthropogenic Inputs are excluded. Reproduced from (Chester, 2009).

	A		B			C		
Element	Fluvial gross flux: total (particulate + dissolved)	Atmospheric flux: total (particulate + soluble)	Fluvial net dissolved flux	Hydrothermal dissolved flux	Atmospheric soluble flux	Fluvial gross particulate flux	Fluvial net particulate flux	Atmospheric particulate flux
Al	54×10^{12}	0.25×10^{12}	$3.5\text{-}6.0 \times 10^{10}$	$1.2\text{-}6.0 \times 10^8$	1.2×10^{10}	54×10^{12}	5.4×10^{12}	0.24×10^{12}
Fe	13.3×10^{12}	0.065×10^{12}	$0.54\text{-}2.3 \times 10^{10}$	$2.3\text{-}19 \times 10^{10}$	0.49×10^{10}	13×10^{12}	1.3×10^{12}	0.06×10^{12}
Mn	30×10^{12}	0.14×10^{10}	$0.49\text{-}0.55 \times 10^{10}$	$1.1\text{-}3.4 \times 10^{10}$	0.05×10^{10}	0.29×10^{12}	0.029×10^{12}	0.001×10^{10}
Ni	2.4×10^{12}	$<0.12 \times 10^{10}$	0.05×10^{10}	—	$<0.05 \times 10^{10}$	2×10^{10}	0.23×10^{10}	$<0.075 \times 10^{10}$
Co	0.56×10^{12}	0.004×10^{10}	$0.011\text{-}0.013 \times 10^{10}$	$6.6\text{-}68 \times 10^5$	1×10^7	0.52×10^{10}	0.05×10^{10}	0.003×10^{10}
Cr	3.1×10^{12}	$<0.10 \times 10^{10}$	0.036×10^{10}	—	$<0.01 \times 10^{10}$	3×10^{10}	0.3×10^{10}	$<0.09 \times 10^{10}$
V	5.2×10^{12}	$<0.07 \times 10^{10}$	0.07×10^{10}	—	$<0.02 \times 10^{10}$	5×10^{10}	0.5×10^{10}	$<0.05 \times 10^{10}$
Cu	2.5×10^{12}	0.06×10^{10}	$0.1\text{-}0.5 \times 10^{10}$	$3\text{-}13 \times 10^8$	2×10^8	2.4×10^{10}	0.24×10^{10}	0.04×10^{10}
Pb	0.75×10^{12}	0.13×10^{10}	$0.2\text{-}1.5 \times 10^8$	$2.7\text{-}110 \times 10^5$	4×10^8	0.75×10^{10}	0.075×10^{10}	0.09×10^{10}
Zn	6.0×10^{12}	0.31×10^{10}	$0.04\text{-}1.4 \times 10^{10}$	$0.12\text{-}0.32 \times 10^{10}$	0.14×10^{10}	6×10^{10}	0.6×10^{10}	0.17×10^{10}
Cd	0.15×10^{12}	$<0.03 \times 10^9$	3×10^7	—	$<2 \times 10^7$	0.14×10^9	0.014×10^9	$<0.7 \times 10^9$

2. Materials and Methods

2.1 Study Site

The Nakdong River is the longest in South Korea (here abbreviated to Korea) with a 510.4 km length main channel and a watershed area of approximately 23,700 km² (Jeong et al., 2007). The river starts from the eastern part of Korea, heading towards the south, passes Busan, the second-largest city in Korea, and finally enters the South Sea. The mean annual precipitation of the river is 1,253 mm, and most of the rainfall (60-70%) is concentrated during late July to mid-September, owing to summer monsoon and typhoons (Jeong et al., 2007).

The Nakdong River is a significant source of water supplies around Korea's southeastern part for agricultural and civil uses. The anthropogenic exploitation of water leads to the potential possibility of pollution of REEs and trace metals in estuarine waters. To prevent saltwater intrusion, regulate the water level, and manage the water supplies around cities where the river passes through, an estuarine dam was constructed at the river mouth in 1987. The earth core rockfill dam in the Nakdong River currently supplies 7.5×10^8 m³ of river water annually.

Since the Nakdong River Estuary has a single riverine source (Nakdong River) entering the South Sea of Korea, this site is suitable to investigate the seasonal change of mixing between river water and seawater and its behavior dissolved REEs and trace metals as its consequence. The dam located at the mouth of the river regulating the discharge of river water is considered an appropriate site for examining the influence of a dam on the geochemistry of REEs and trace metals in an estuary.

2.2 Analysis

Figure 4 summarizes the basic schematic diagram of sample analysis. The samples collected at the Nakdong River Estuary was filtered, acidified then stored. For measurement, the samples were concentrated beforehand, then their concentrations were determined. Each of the steps is described in detail below.

2.2.1 Sample Collection

The estuarine water samples were collected at a fixed station located 560m downstream from the dam at the Nakdong River Estuary (Lee and Kim, 2018) (Figure 5). The sampling was conducted once a month from October 2014 to August 2015 (11 months). The samples were collected in high-density polyethylene (HDPE) bottles every hour for 24 hours during spring tide using an autosampler (RoboChem™ Autosampler; Centennial Technology, Korea, Model S3-1224N) deployed at 1m below the surface (Lee and Kim, 2018). The HDPE bottles were prepared to be trace metal-clean beforehand to prevent any possibility of contamination. HDPE bottles were soaked in 65°C 5% HNO₃ (Ultrapure grade) for 2 hours and cleaned thoroughly using de-ionized water (DIW) five times. The bottles were stored in double-packed plastic bags, which also had gone through the same cleaning process with HDPE bottles. Once the samples were collected, they were immediately carried to a trace metal-clean laboratory (Class-100) within 24 hours. All estuarine samples were filtered with 0.45µm filters (mixed cellulose ester, Advantech) then acidified below pH two using double-distilled 6M HNO₃ for long term storage. The salinity of each sample was measured using a YSI Pro Series conductivity probe sensor in the laboratory.

2.2.2 Preconcentration of Rare Earth Elements and Trace Metals

The acidified Nakdong River estuarine water samples were transferred to HDPE conical tubes for measurement. To prevent the tubes' potential contamination, they were soaked in detergent for at least 12 hours and washed with DIW seven times. After removing the detergent, the tubes were soaked in 5% HNO₃ (Ultrapure grade) for at least 24 hours, then washed again with DIW. Lastly, the tubes were submerged in 5% HNO₃ (Ultrapure grade), heated up to 65°C for 2 hours, washed with DIW, then thoroughly dried in a dust-free, trace metal-clean bench (Class-100) until the DIW is fully vaporized. 10mL of river water samples were moved from HDPE bottles to prepared conical tubes for analysis.

Since REEs and trace metals are present at low concentrations, the sample must be concentrated beforehand in trace-metal clean conditions for accurate measurement. A commercial system (seaFAST SP3 system, ESI) was used to concentrate the REEs and trace metals in the sample and remove major ion matrix to avoid potential interference during instrumental analysis in pristine condition. Even though seaFAST is typically used to analyze seawater, it can still be utilized in the sample with a high matrix such as riverine waters. The preconcentration by seaFAST was done in a clean enclosed unit equipped with air filters. The seaFAST system uses chelation resin columns to conduct the preconcentration processes. The three major steps demonstrate the procedure: (1) loading of samples, (2) rinsing off major ion matrix, and (3) elution of REEs and trace metals (Figure 6a). The autosampler probe fills the sample coil with 10mL of the acidified sample by suction. While the sample stays in the resin column, the sample's pH is adjusted to 6.0 ± 0.2 with 4 M NH₄Ac buffer (ESI), and the salt and major ion matrix are removed with DIW (Kohler, 2017; Rapp et al., 2017). Then, the sample-buffer solution is moved

to the chelation column, which was preconditioned in 0.1% HNO₃ (Ultra High Pure Grade, ODLAB), and is eluted with 8% HNO₃ (Rapp et al., 2017). The chelation column used for preconcentration is filled with Nobias-chelate PA1 resin, the hydrophilic methacrylate polymer on which ethylenediaminetriacetic and iminodiacetic acids are immobilized (Sohrin et al., 2008) (Figure 6b). This resin is known to have an excellent affinity for trace metals by forming up to five coordinating bonds with metal ions with its chelating group (Sohrin et al., 2008). After separated and the matrix is removed, the samples are directly injected into the nebulizer of the analytical instrument, and the column is rinsed and conditioned for the next sample with buffer and DIW (Rapp et al., 2017).

2.2.3 Instrumental Analysis

In this study, high-resolution sector field inductively coupled plasma mass spectrometry (HR-SF-ICP-MS; Element II™, Thermo Fisher Scientific) was used to determine both REEs and trace metals. All 14 elements of REEs (La to Lu) and eight trace metals (Fe, Mn, V, Co, Ni, Cu, Cd, and Mo) were measured. ICP-MS applies inductively coupled plasma to generate atomic ions from samples, which are then measured in the form of a mass-to-charge ratio (Figure 7). The instrument provides three resolution modes: (1) low-resolution mode (LR), (2) middle-resolution mode (MR), and (3) high-resolution mode (HR). Not all elements require HR for measurement, so REEs trace metals were analyzed in LR and MR, respectively. The instrument's sensitivity was checked with three elements ⁷Li, ¹¹⁵In, ²³⁸U by using a tuning solution (1 µg/L) from Thermo Fisher scientific in LR mode. The minimum counts for each element were 1.0×10⁶, 2.0×10⁷, and 3.5×10⁷. Since ICP-MS has the possibility of interference by Ar gas, air, contamination, and solvent of the sample,

it should be confirmed that the interference does not interrupt accurate analysis of elements. The count of ^{151}Eu and $^{135}\text{Ba}^{16}\text{O}$ was compared in LR mode to ensure that the count of $^{135}\text{Ba}^{16}\text{O}$ does not exceed more than 0.3% of ^{151}Eu , and the interference of $^{40}\text{Ar}^{16}\text{O}$ on ^{56}Fe was examined in MR every time before measurement for higher accuracy. When measuring trace metals, interference between Mo and Cd was also considered; some portion of Mo could be detected as Cd due to the oxidized form of Mo (MoO^+). Cd-free Mo standards were measured to make a linear regression curve to correct the measured values by subtracting the count of Cd that has increased by oxidized Mo. To monitor the consistency of the process, Rh was spiked as an internal standard in each sample. Also, certified reference material (CRM; SLRS-4, National Research Council of Canada) was analyzed for confirmation. Furthermore, to continually check the sensitivity of ICP-MS, standards with the highest concentration or CRM were measured for every five samples to test the count of elements. If the result fluctuated within $\pm 5\%$, the measurement proceeded. The machine was washed with 1% HNO_3 for 210 seconds between each sample to prevent the memory effect of ICP-MS. The instruments used in this study (SeaFAST system connected to HR-ICP-MS) can be seen in Figure 8. The operating condition of ICP-MS, correspondence of CRM with known values, and the detection limit of REEs and trace metals are presented in Table 2, Table 3, and Table 4. The determined values which were below the detection limit were omitted.

2.2.4 Data Collection and Quality Control

Since the samples were collected 5 to 6 years ago, there were some lost samples when the analysis was in progress. There are samples collected for nutrient analysis, and the suitability for measuring REEs and trace metals should be tested. Among the

total 264 samples gathered throughout the sampling period, only 137 samples were available for analysis. Also, despite the effort to prevent possible contamination during sampling and storage, some samples were excluded due to contamination. Some months could not cover the time range between ebb to flow (12 hours) during the sampling period owing to the loss of samples, and these months were considered deficient in explaining the mixing of saltwater intrusion and riverine discharge fully. Data from three months (February, March, and June) were omitted in evaluating the monthly behavior of REEs and trace metals. Even though the full set of samples were not analyzed, the data seems to be adequate for evaluation since the data covers the period of sampling over the whole season. The real-time data of discharge volume from the Nakdong River Estuary dam are accessible at Mywater (<http://www.water.or.kr/>) or Nakdong River Flood Control Office (<http://www.nakdongriver.go.kr/main.do>).

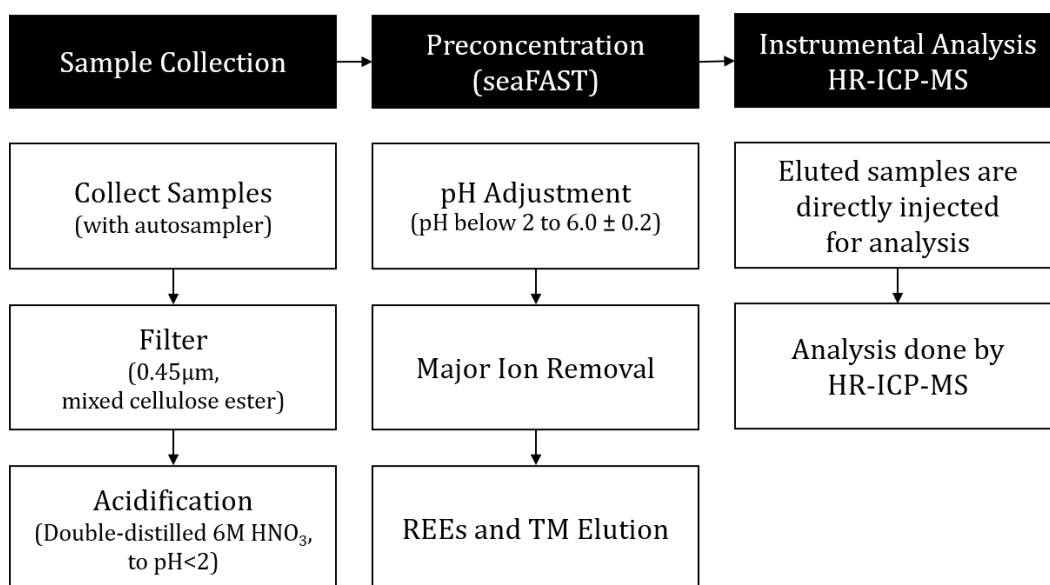


Figure 4. Schematic diagrams of the overall analytical procedure for rare earth elements and trace metals.

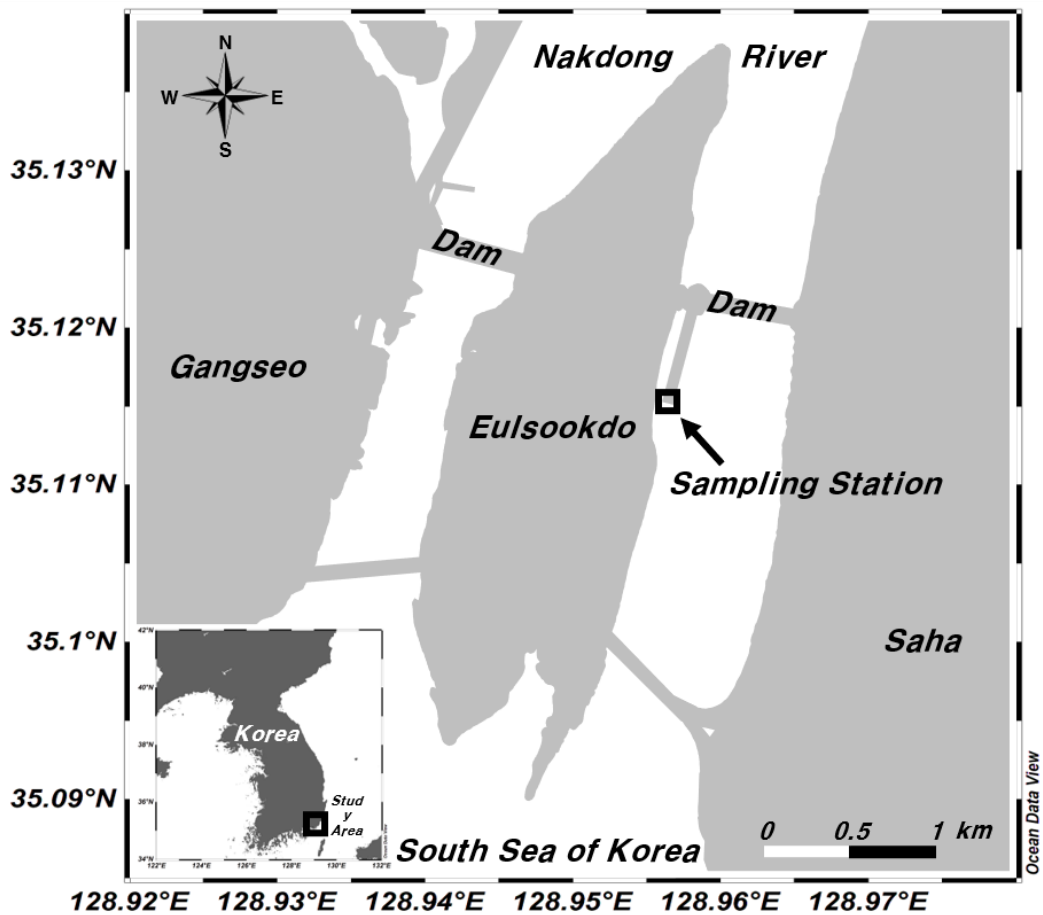


Figure 5. Location of sampling station in the Nakdong River Estuary.

Modified from (Lee and Kim, 2018).

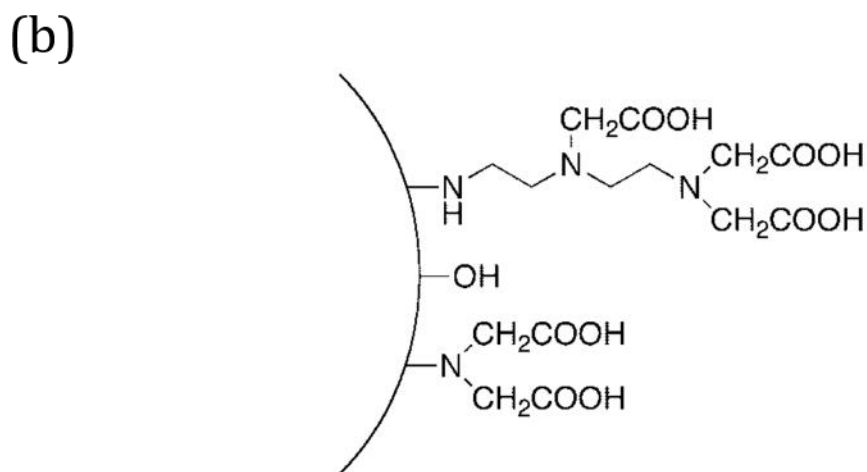
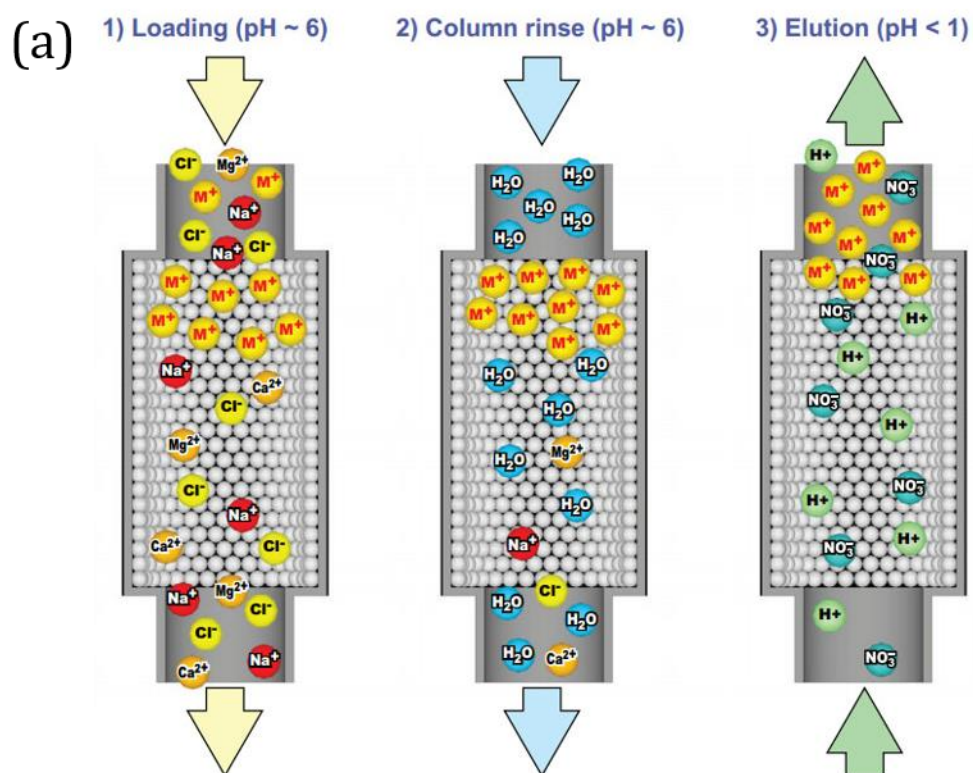


Figure 6. (a) Schematic overview of the seaFAST preconcentration column. Reproduced from Elemental Scientific. (b) Chemical structure of functional groups on Nobias Chelate-PA1. Reproduced from (Sohrin et al., 2008).

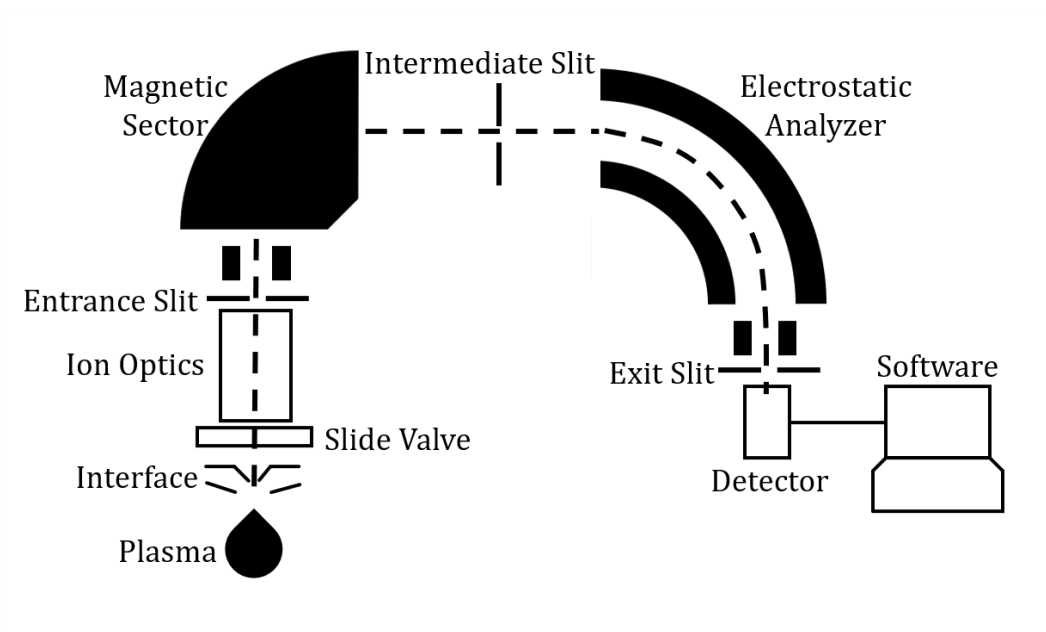


Figure 7. Schematic overview of the high resolution inductively coupled plasma mass spectrometry (HR-ICP-MS). Modified from (Jakubowski et al., 1998).



Figure 8. Instruments used in this study: SeaFAST SP3 system (right) connected to high resolution inductively coupled plasma mass spectrometry (HR-ICP-MS) (left).

Table 2. Operating conditions for high resolution inductively coupled plasma mass spectrometry (HR-ICP-MS).

HR-ICP-MS (Thermo Element II TM)	
Plasma Condition	
Forward power	1250 [W]
Cool gas flow	16.00 [L·min ⁻¹]
Auxiliary Ar flow	0.7 - 0.8 [L·min ⁻¹]
Nebulizer	
Ar gas flow	1.016 [L·min ⁻¹]
Peristaltic pump speed	10 [rpm]
Data Acquisition	
Quantification type	Intensities [cps]
Acquisition time	80 [s]

Table 3. Measured values of rare earth elements and trace metals for certified reference materials (SLRS-4 and CASS-6).

(a) (Yeghicheyan et al., 2001), n=174

(b) (Ma et al., 2019), n=2

Elements	SLRS-4 (n=12) [pM]		CASS-6 (n=6) [pM]		Elements	SLRS-4 (n=10) [nM]	
	(a)	This Study	(b)	This Study		(a)	This Study
La	287 ± 8	287.7 ± 20.9	9.1 ± 0.1	10.1 ± 0.18	V	0.32 ± 0.03	0.33 ± 0.02
Ce	360 ± 12	362.0 ± 26.9	5.9 ± 0.2	5.6 ± 0.07	Mn	3.37 ± 0.18	3.13 ± 0.44
Pr	69.3 ± 1.8	67.5 ± 5.2	1.3 ± 0.1	1.6 ± 0.04	Fe	103 ± 5	100.92 ± 7.66
Nd	269 ± 14	234.8 ± 18.1	5.5 ± 0.1	5.5 ± 0.07	Co	0.033 ± 0.006	0.03 ± 0.01
Sm	57.4 ± 2.8	55.8 ± 4.1	1 ± 0.03	1.2 ± 0.05	Ni	0.67 ± 0.08	0.65 ± 0.09
Eu	8.0 ± 0.6	8.0 ± 0.6	0.3 ± 0.02	0.5 ± 0.04	Cu	1.81 ± 0.08	1.68 ± 0.19
Gd	34.2 ± 2.0	40.8 ± 3.4	1.6 ± 0.05	1.9 ± 0.05	Cd	0.012 ± 0.002	0.02 ± 0.01
Tb	4.3 ± 0.4	5.2 ± 0.4	0.2 ± 0.03	0.4 ± 0.08	Mo	0.21 ± 0.02	0.28 ± 0.13
Dy	24.2 ± 1.6	23.6 ± 1.8	1.1 ± 0.03	1.6 ± 0.06			
Ho	4.7 ± 0.3	4.9 ± 0.3	0.3 ± 0.01	0.5 ± 0.04			
Er	13.4 ± 0.6	14.1 ± 1.1	0.9 ± 0.01	1.3 ± 0.07			
Tm	1.7 ± 0.2	2.2 ± 0.2	0.1 ± 0.01	0.4 ± 0.07			
Yb	12.0 ± 0.4	12.5 ± 0.8	1 ± 0.2	1.5 ± 0.07			
Lu	1.9 ± 0.1	2.3 ± 0.1	0.2 ± 0.01	0.6 ± 0.12			

Table 4. Reagent blanks and instrument detection limits of rare earth elements (n=9) and trace metals (n=12)

Elements	m/z	Blank [ng·L ⁻¹]	D.L. [ng·L ⁻¹]	Elements	m/z	Blank [ng·L ⁻¹]	D.L. [ng·L ⁻¹]
La	139	0.04	0.06	V	51	0.01	14.88
Ce	140	0.07	0.16	Mn	55	2.49	9.06
Pr	141	0.09	0.19	Fe	56	1.20	12.55
Nd	144	0.06	0.16	Co	59	1.19	10.86
Sm	147	0.05	0.15	Ni	60	2.89	15.57
Eu	153	0.09	0.20	Cu	63	0.06	11.16
Gd	157	0.07	0.21	Cd	111	2.28	6.29
Tb	159	0.05	0.25	Mo	95	1.27	22.81
Dy	163	0.06	0.25				
Ho	165	0.07	0.13				
Er	166	0.08	0.10				
Tm	169	0.13	0.03				
Yb	172	0.11	0.22				
Lu	175	0.14	0.23				

3. Results

3.1. Rare Earth Elements

3.1.1. Distributions of Dissolved Rare Earth Elements

Figure 9 presents the concentration of dissolved REEs against salinities. Eight elements represent the REEs as they have similar distribution due to their coherent chemical properties. The salinity of the samples ranged from 0.2 to 25.9. The dissolved REE concentrations varied by up to two orders of magnitude; La ranged from 24 pM to 251 pM while Lu ranged between 2.6 pM and 8.0 pM (Table 5).

The elements showed a linear correlation with salinity, which coincided with the conservative mixing line of river water and seawater endmember. Although the elements were similar to each other, the slope of each element displayed systematic changes. The LREEs showed a positive linear correlation with increasing salinity, while heavier elements such as Er to Lu showed constant and even negative correlation (Yb and Lu). Since the seawater endmember concentration in this study corresponds with previously reported data in November 2017 (Kim et al., 2020), the altering trend among the REEs appears to result from varying river water endmember concentration.

However, unlike the other months, data from October, April, and July demonstrated a highly non-conservative trend with respect to the mixing of freshwater and seawater. In the low-salinity region, the concentrations of the three months showed wide scatter and were approximately 2 to 12-folds greater compared to the extrapolated riverine endmember concentration of the conservative mixing line. The concentration showed less scattered distribution in the mid to high-salinity

region and showed conservative mixing between riverine endmember and seawater endmember as the concentrations approached the seawater endmember.

Apart from the systematic changes, a distinctive element showed a trend that did not conform well with adjacent elements. Gd showed a conservative decline with increasing salinity, unlike other MREEs, which showed a positive correlation with increasing salinity and anomalous three months. The Gd-salinity distribution appears to resemble the trend of heavy elements such as Yb and Lu. Several data from October also showed higher concentration compared to the freshwater–seawater mixing line.

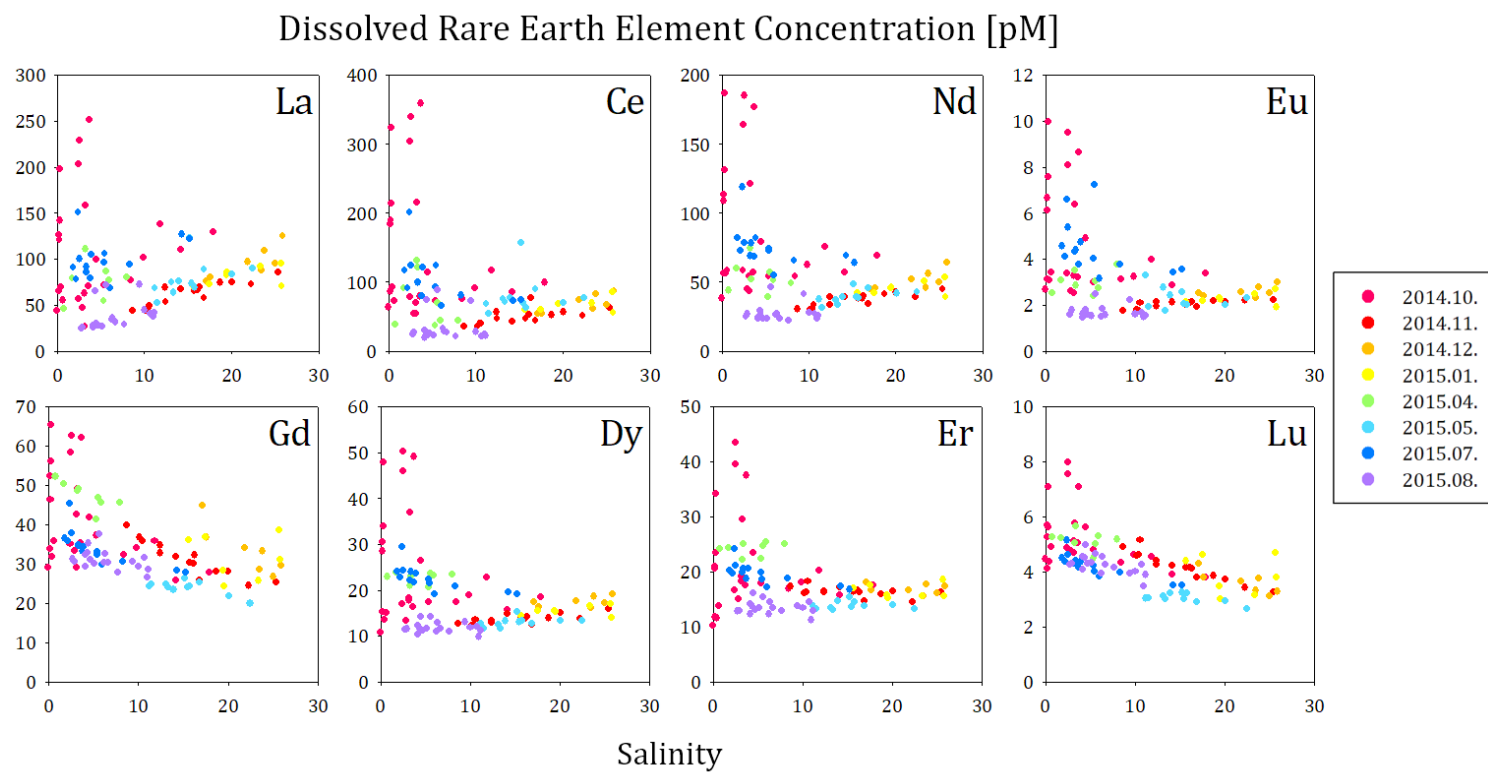


Figure 9. Graphs of dissolved rare earth elements versus salinities in the Nakdong River Estuary.

Table 5. Concentrations of rare earth elements against salinities. (N.D.: Not Detected)

Sampling Time	Salinity	Concentrations of Rare Earth Elements [pM]													
		La	Ce	Pr	Nd	Sm	Eu	Gd	Tb	Dy	Ho	Er	Tm	Yb	Lu
2014-10-23 15:00	0.2	120.8	189.3	27.1	108.8	26.1	6.1	46.3	4.7	28.5	6.5	21.0	3.5	28.3	5.7
2014-10-23 16:00	0.3	197.8	324.3	47.1	187.0	43.9	10.0	65.3	7.7	48.0	10.9	34.1	5.2	37.8	7.1
2014-10-23 17:00	0.4	69.9	93.4	14.6	56.5	12.9	3.1	31.9	2.3	13.6	3.3	11.6	2.3	20.6	4.4
2014-10-23 18:00	0.2	65.3	86.4	14.3	56.6	13.3	3.1	33.9	2.4	15.3	3.6	11.7	2.0	18.2	4.1
2014-10-23 19:00	0.2	43.8	63.5	10.0	38.3	9.8	2.7	29.0	2.0	10.8	3.0	10.2	2.2	19.6	4.5
2014-10-23 20:00	0.3	141.9	213.6	33.2	131.3	32.3	7.6	56.0	5.7	33.9	7.5	23.4	3.7	27.7	5.6
2014-10-23 21:00	0.2	126.5	184.0	28.8	113.3	28.8	6.7	52.5	5.1	30.5	6.7	20.6	3.2	25.6	5.3
2014-10-23 22:00	0.6	55.2	73.0	14.0	58.6	14.6	3.4	35.9	2.5	15.1	3.7	13.9	2.7	24.5	4.9
2014-10-23 23:00	4.5	99.3	113.8	19.4	79.1	19.4	4.9	41.8	4.2	26.5	6.7	23.4	4.1	29.1	5.6
2014-10-24 1:00	2.5	229.0	339.3	47.7	185.2	40.9	9.5	62.7	7.5	50.2	12.8	43.5	6.8	47.4	8.0
2014-10-24 2:00	3.2	27.2	54.3	9.7	43.3	10.5	2.5	29.0	2.3	18.2	5.0	19.2	3.3	25.5	4.7
2014-10-24 3:00	3.7	251.6	358.8	45.6	177.2	38.5	8.7	62.0	7.2	49.1	11.6	37.5	5.9	40.7	7.1
2014-10-24 4:00	3.3	158.2	215.6	30.0	121.3	27.3	6.4	49.1	5.5	37.0	8.9	29.5	4.6	32.7	5.8
2014-10-24 5:00	2.5	203.3	304.6	42.1	163.9	35.6	8.1	58.3	6.5	46.0	11.5	39.6	6.3	44.0	7.5
2014-10-24 6:00	2.4	56.8	78.8	13.9	58.6	14.0	3.4	35.1	2.7	17.0	4.3	16.6	3.1	25.2	4.9
2014-10-24 7:00	2.9	47.1	54.7	10.5	45.1	11.2	2.6	33.4	2.1	13.4	3.6	15.1	2.9	24.2	4.8
2014-10-24 8:00	3.6	70.3	79.3	13.9	57.0	13.5	3.2	35.4	2.6	16.4	4.3	17.6	3.2	25.7	5.1
2014-10-24 9:00	8.4	76.7	75.4	13.3	54.3	12.7	3.1	32.3	2.5	17.4	4.5	16.9	3.0	22.7	4.3
2014-10-24 10:00	9.9	101.6	91.5	15.7	62.4	13.6	3.2	34.2	2.7	18.9	4.8	18.2	3.1	24.1	4.6
2014-10-24 11:00	17.9	129.2	99.3	18.5	69.4	13.9	3.4	27.9	2.9	18.5	4.8	17.6	2.8	20.9	3.8
2014-10-24 12:00	14.2	110.0	85.7	14.8	57.1	11.5	2.9	25.7	2.4	15.7	4.2	15.7	2.7	20.0	3.9
2014-10-24 13:00	11.8	138.4	116.9	19.8	75.8	16.2	4.0	35.8	3.4	22.8	5.8	20.2	3.3	24.4	4.5
2014-10-24 14:00	5.4	71.8	73.5	13.0	54.0	12.7	3.0	37.2	2.6	17.4	4.6	18.0	3.2	25.3	4.8
2014-10-24 15:00	3.1	62.7	70.1	12.7	54.2	13.6	3.3	42.7	2.7	17.7	4.5	18.3	3.3	27.2	5.1
2014-11-24 15:00	18.7	74.5	52.1	10.9	41.7	8.6	2.2	28.2	2.0	13.9	4.0	16.0	2.7	20.9	3.9
2014-11-24 17:00	16.8	58.0	44.3	8.9	34.2	7.5	1.9	25.9	1.7	12.5	3.7	14.7	2.7	20.7	3.8

Table 5. Concentrations of rare earth elements against salinities (Continued).

Sampling Time	Salinity	Concentrations of Rare Earth Elements [pM]													
		La	Ce	Pr	Nd	Sm	Eu	Gd	Tb	Dy	Ho	Er	Tm	Yb	Lu
2014-11-24 23:00	22.3	72.4	52.0	10.4	39.3	N.D.	2.2	24.4	2.0	13.9	3.9	14.5	2.5	18.8	3.4
2014-11-25 1:00	15.7	65.3	47.7	9.8	38.2	8.4	2.0	30.3	1.8	13.8	4.1	16.4	2.9	22.5	4.2
2014-11-25 2:00	16.1	66.7	52.9	9.9	38.2	8.2	2.1	30.1	1.8	13.7	4.1	16.6	2.9	22.5	4.2
2014-11-25 3:00	14.2	67.2	43.4	9.9	39.6	8.6	2.1	31.8	1.9	14.9	4.2	17.2	3.0	23.5	4.2
2014-11-25 4:00	12.4	69.0	56.4	10.2	39.5	8.7	2.1	32.7	1.8	13.4	3.9	16.4	2.9	22.9	4.3
2014-11-25 5:00	10.6	49.5	39.7	8.5	33.7	7.9	2.1	N.D.	6.6	13.6	4.3	18.2	3.6	27.0	5.2
2014-11-25 6:00	10.4	46.7	39.4	7.6	30.4	7.1	1.7	35.8	N.D.	12.2	3.8	16.3	3.1	24.3	4.6
2014-11-25 7:00	8.7	43.8	36.0	7.5	30.4	7.1	1.8	39.9	1.7	12.7	3.9	17.3	3.1	25.7	4.9
2014-11-25 8:00	10.2	44.0	35.9	7.6	30.1	6.9	1.8	36.7	1.6	12.3	3.7	16.2	3.0	24.7	4.6
2014-11-25 9:00	12.4	53.1	46.6	8.6	33.8	7.6	1.9	34.7	1.8	12.8	3.8	16.5	3.0	23.8	4.4
2014-11-25 10:00	16.3	69.3	77.4	10.4	39.9	9.1	2.1	32.2	1.9	14.3	3.9	16.4	2.8	22.5	4.1
2014-11-25 12:00	25.4	85.3	63.0	11.8	44.9	9.0	2.2	25.3	2.1	15.9	4.3	16.3	2.6	18.9	3.3
2014-11-25 13:00	20.0	74.8	56.4	10.9	42.5	9.3	2.1	28.2	2.0	15.0	4.2	16.5	2.7	21.1	3.7
2014-12-22 17:00	17.6	80.7	53.8	11.7	45.8	9.8	2.4	36.7	2.2	16.3	4.4	16.7	2.8	21.4	3.8
2014-12-22 19:00	17.1	76.5	54.1	11.7	44.9	10.2	2.5	44.8	2.3	17.4	4.7	18.0	3.1	23.4	4.3
2014-12-22 23:00	21.8	96.9	74.7	13.8	52.1	11.1	2.6	34.1	2.4	17.7	4.7	16.7	2.7	20.5	3.7
2014-12-23 3:00	23.8	109.2	83.4	14.4	56.1	11.5	2.8	33.2	2.6	18.6	4.9	17.7	2.8	21.0	3.8
2014-12-23 5:00	25.9	125.1	87.3	16.7	64.5	13.0	3.0	29.6	2.8	19.2	4.9	17.3	2.6	19.1	3.3
2014-12-23 7:00	25.0	95.1	67.4	13.1	49.9	10.2	2.5	26.7	2.3	17.2	4.5	16.1	2.5	18.5	3.1
2014-12-23 13:00	23.5	87.5	61.8	12.0	46.1	9.3	2.3	28.5	2.2	16.1	4.3	15.6	2.5	18.8	3.3
2015-1-21 15:00	25.7	95.2	85.9	14.6	53.3	11.6	2.7	38.6	2.4	17.0	4.7	18.6	3.2	25.1	4.7
2015-1-21 17:00	17.5	72.6	60.5	10.8	42.4	9.3	2.2	36.9	2.0	15.5	4.4	17.5	3.1	24.6	4.6
2015-1-21 19:00	15.6	70.0	59.8	11.2	42.2	9.0	2.2	36.0	2.0	14.3	4.3	17.1	3.0	23.3	4.4
2015-1-21 23:00	19.5	85.9	68.5	12.2	46.1	9.2	2.3	24.3	2.1	15.2	4.1	15.2	2.3	17.2	3.0
2015-1-22 3:00	25.7	70.3	55.4	10.0	39.2	8.2	1.9	31.0	1.9	14.1	3.9	15.6	2.6	20.3	3.8
2015-1-22 5:00	23.3	92.0	69.3	13.3	50.6	10.3	2.5	25.7	2.3	16.5	4.3	15.6	2.5	18.2	3.1

Table 5. Concentrations of rare earth elements against salinities (Continued).

Sampling Time	Salinity	Concentrations of Rare Earth Elements [pM]													
		La	Ce	Pr	Nd	Sm	Eu	Gd	Tb	Dy	Ho	Er	Tm	Yb	Lu
2015-1-22 7:00	19.4	83.0	69.0	12.0	45.6	9.4	2.3	28.3	2.1	15.4	4.2	15.7	2.6	19.5	3.5
2015-4-21 11:00	5.3	54.3	37.7	9.6	39.4	10.0	2.4	41.3	2.4	20.6	5.9	22.5	3.6	26.5	4.5
2015-4-21 19:00	0.8	46.2	38.2	10.9	43.9	11.2	2.5	52.2	2.7	22.9	6.6	24.2	3.9	29.9	5.3
2015-4-21 21:00	1.7	79.2	91.3	16.3	60.1	14.3	3.1	50.4	3.0	23.9	6.6	24.4	3.9	29.3	5.2
2015-4-21 23:00	5.6	86.7	69.4	15.3	57.1	13.3	3.1	46.9	2.9	23.7	6.7	24.6	3.9	28.9	5.0
2015-4-22 3:00	7.9	80.5	44.2	12.5	49.5	11.6	3.8	45.5	2.8	23.4	6.8	25.0	4.1	30.2	5.2
2015-4-22 5:00	5.9	77.2	44.9	12.6	51.1	12.1	2.7	45.6	2.8	23.2	6.8	25.4	4.0	29.7	5.3
2015-4-22 7:00	3.3	110.8	131.9	21.0	74.7	16.6	3.5	48.6	2.9	21.0	5.9	22.3	3.8	28.1	5.0
2015-4-22 9:00	3.3	85.9	121.1	13.4	52.2	13.0	2.8	49.2	2.9	22.9	6.6	25.0	4.2	31.6	5.6
2015-5-19 17:00	13.9	76.5	76.8	10.5	39.1	8.1	2.4	23.5	1.8	13.2	3.8	14.7	2.5	17.8	3.2
2015-5-19 19:00	13.3	63.7	71.7	8.8	33.9	7.0	1.8	24.0	N.D.	11.6	3.4	13.1	2.3	16.8	3.0
2015-5-19 21:00	15.5	73.3	69.4	10.6	39.4	8.2	2.1	24.1	1.7	13.0	3.7	13.7	2.4	17.2	3.0
2015-5-19 23:00	16.8	88.9	90.2	12.9	45.6	8.9	N.D.	25.3	1.8	12.6	3.7	13.8	2.3	16.7	2.9
2015-5-20 1:00	15.8	69.1	62.6	10.4	38.5	8.3	2.0	24.3	1.8	13.3	3.8	14.6	2.4	17.4	3.2
2015-5-20 3:00	15.2	122.8	157.4	13.5	48.7	10.0	2.6	26.2	2.1	15.3	4.2	15.4	2.4	18.3	3.2
2015-5-20 5:00	13.1	74.9	76.3	9.9	36.9	8.0	2.8	24.8	1.7	12.5	3.5	13.5	2.3	16.5	3.1
2015-5-20 7:00	11.5	52.6	54.3	8.0	31.2	7.3	1.9	24.9	1.6	11.7	3.5	13.3	2.3	17.7	3.0
2015-5-20 9:00	11.2	68.9	68.2	9.9	37.5	7.8	3.3	24.4	1.7	12.7	3.6	13.7	2.3	17.0	3.0
2015-5-20 11:00	20.1	83.4	69.5	11.4	41.9	8.8	2.0	21.9	1.8	13.4	3.8	13.9	2.2	16.8	2.9
2015-5-20 13:00	22.4	89.7	77.5	11.8	42.9	8.5	2.3	20.0	1.9	13.4	3.7	13.3	2.1	15.4	2.6
2015-7-15 12:00	6.0	68.6	66.3	13.1	54.8	12.7	3.2	29.9	2.8	19.1	4.8	17.1	2.8	21.1	3.8
2015-7-15 14:00	2.4	150.6	200.7	31.8	118.8	26.7	6.6	45.3	4.6	29.4	6.9	24.2	4.0	28.7	5.1
2015-7-15 15:00	1.8	90.7	117.3	20.6	81.9	19.8	4.6	36.5	3.6	24.1	5.9	20.3	3.3	24.9	4.5
2015-7-15 16:00	2.2	78.5	91.9	17.7	73.0	17.9	4.1	35.9	3.5	22.8	5.7	19.7	3.3	24.3	4.4
2015-7-15 17:00	2.5	100.2	124.2	19.7	78.6	18.5	5.4	37.9	3.6	24.3	6.0	21.1	3.5	26.4	4.6
2015-7-15 18:00	3.3	85.9	99.3	16.9	68.8	16.4	4.3	34.8	3.2	22.2	5.6	19.9	3.3	24.6	4.3

Table 5. Concentrations of rare earth elements against salinities (Continued).

Sampling Time	Salinity	Concentrations of Rare Earth Elements [pM]													
		La	Ce	Pr	Nd	Sm	Eu	Gd	Tb	Dy	Ho	Er	Tm	Yb	Lu
2015-7-15 19:00	3.8	78.8	79.5	16.6	68.7	16.3	3.8	33.2	3.1	21.7	5.4	18.7	3.1	23.1	4.1
2015-7-15 20:00	5.4	105.9	124.0	19.4	74.4	16.7	7.3	32.4	3.2	21.4	5.3	18.6	3.1	23.0	4.0
2015-7-15 22:00	15.2	122.3	74.7	16.6	63.8	13.7	3.6	27.9	2.7	19.1	4.8	16.7	2.7	19.9	3.5
2015-7-15 23:00	14.3	126.9	73.2	17.5	69.3	14.4	3.4	28.4	2.9	19.5	5.0	17.4	2.8	20.2	3.5
2015-7-16 0:00	8.3	94.2	80.7	16.3	65.7	15.1	3.8	30.5	3.0	20.9	5.2	18.8	3.0	22.2	4.0
2015-7-16 1:00	5.4	96.2	92.8	18.1	73.1	16.7	4.0	33.0	3.2	22.3	5.6	19.9	3.2	23.7	4.2
2015-7-16 2:00	3.9	105.2	121.9	21.5	82.2	19.0	4.7	34.3	3.6	23.7	5.8	20.6	3.3	24.6	4.4
2015-7-16 3:00	3.4	91.4	99.9	18.8	78.1	18.9	4.4	34.7	3.6	24.0	5.9	20.6	3.3	24.6	4.4
2015-8-26 12:00	2.9	26.2	27.6	6.1	26.8	7.0	1.8	30.5	N.D.	11.5	3.2	12.9	2.5	21.7	4.3
2015-8-26 14:00	2.7	24.7	24.3	5.7	25.0	6.6	1.6	31.2	N.D.	11.4	3.2	12.8	2.4	20.8	4.3
2015-8-26 16:00	4.1	27.8	30.0	5.7	23.6	5.8	1.5	29.4	N.D.	10.3	3.0	12.3	2.4	19.9	4.1
2015-8-26 17:00	4.4	65.3	74.6	8.8	29.1	6.9	1.7	32.9	1.6	11.6	3.3	13.7	2.6	22.0	4.5
2015-8-26 18:00	4.7	27.7	26.2	5.6	23.7	6.3	1.6	31.2	N.D.	11.3	3.2	13.0	2.5	21.3	4.3
2015-8-26 20:00	6.2	33.9	33.0	6.6	26.6	6.3	1.5	30.4	N.D.	11.0	3.0	12.3	2.3	19.7	3.9
2015-8-26 21:00	11.0	37.8	23.7	5.8	23.5	5.6	1.5	26.7	N.D.	9.8	2.8	11.2	2.0	17.5	3.5
2015-8-26 22:00	9.4	72.2	72.3	11.5	41.5	9.5	2.2	30.7	1.8	13.0	3.4	13.8	2.4	20.6	3.9
2015-8-26 23:00	6.7	31.6	27.4	5.7	23.7	6.3	1.6	30.3	N.D.	11.6	3.2	13.4	2.5	21.5	4.3
2015-8-27 0:00	7.7	29.1	21.3	5.4	22.4	5.2	N.D.	27.8	N.D.	11.0	3.2	12.9	2.4	20.7	4.2
2015-8-27 1:00	5.1	27.0	23.3	5.3	23.5	5.9	1.5	30.1	N.D.	11.6	3.3	13.4	2.5	21.9	4.3
2015-8-27 2:00	4.2	25.4	19.5	5.4	24.1	6.2	1.6	32.4	1.6	12.2	3.4	14.2	2.7	22.8	4.5
2015-8-27 4:00	4.4	30.0	22.4	6.3	27.2	7.2	1.8	35.2	1.8	14.2	3.9	16.2	3.0	24.7	5.0
2015-8-27 5:00	5.6	71.8	89.0	13.1	46.7	10.5	2.5	37.6	2.0	14.2	3.9	15.4	2.9	24.2	4.7
2015-8-27 6:00	6.3	36.4	28.6	6.5	27.4	6.8	1.8	32.7	1.7	12.9	3.6	14.5	2.8	23.2	4.5
2015-8-27 8:00	10.0	44.6	27.9	6.9	28.0	6.6	1.6	29.4	N.D.	11.8	3.3	13.4	2.4	21.0	4.0
2015-8-27 9:00	10.7	40.5	21.9	6.8	27.3	6.5	1.7	31.7	1.6	12.1	3.5	14.5	2.6	22.3	4.3
2015-8-27 10:00	11.1	41.4	22.1	6.3	25.7	6.2	1.5	28.6	N.D.	11.2	3.1	12.9	2.3	19.7	3.9

3.1.2. Shale–Normalized Pattern of Dissolved Rare Earth Elements

The distribution of REEs in nature follows the Oddo-Harkins rule, which is a tendency of the even atomic-numbered elements being more abundant than adjacent odd-numbered elements. This tendency of abundance occurs due to the difference in stability depending on the electron configuration of the elements. In order to determine the fractionation behaviors and anomalies of the elements, the concentrations of REEs are often normalized with reference data sets to eliminate the variation induced by natural abundance. In this study, Post-Archean Australian Shale (PAAS) values were utilized to normalize the measured concentrations. Figure 10 presents the average values of each month (Taylor and McLennan, 1985; Migaszewski and Galuszka, 2015). The normalized REE patterns showed three different traits of the Nakdong River Estuary.

(1) The PAAS values of REEs showed an increasing pattern across the series in all seasons. The average normalized values of HREEs were 5.5-fold greater than that of LREEs. It seems that the fractionation of REEs accompanied the depletion of dissolved LREEs in samples relative to HREEs throughout the sampling period. The comparison with the data reported in the Nakdong River Estuary in November 2017 (Kim et al., 2020) also showed an up to 92% decrease for LREEs while HREEs show a 60% decline.

(2) Depletion of Ce concentration relative to the other REEs was constantly observed around all months. Unlike the other REEs, which have the trivalent state as their dominant form in aquatic solution, Ce is the only element in the series that exists in a tetravalent form. Since Ce^{4+} is less soluble compared to other trivalent REEs, the element usually exists in particulate form and is prone to removal in aqueous solution (Goldberg et al., 1963; de Baar et al., 1985; Elderfield, 1988;

Sholkovitz, 1993). The Ce anomaly (Ce_N/Ce_N^*) was calculated with the following equation (Shields and Stille, 2001):

$$Ce_N/Ce_N^* = 3Ce_N / (2La_N + Nd_N) \quad (1)$$

The subscript N and superscript * each denotes the PAAS normalized form of dissolved REE concentration and estimated natural concentration by interpolating adjacent elements. Calculated Ce anomaly value indicates the accordance with the crustal composition of PAAS. When the value is between 0 and 1, it is called 'negative' Ce anomaly meaning that fractionation has occurred from its adjacent elements through deficiency of Ce by geochemical reactions depending on the surrounding environment. In this study, the Ce anomaly value ranged from 0.27 to 0.76. Negative anomalies (0.1-0.5) are generally reported in seawater where removal of tetravalent Ce occurs (Elderfield, 1988; Sholkovitz and Schneider, 1991; Piepgras and Jacobsen, 1992; Sholkovitz, 1993).

(3) Positive Gd anomalies were observed consistently throughout the whole sampling period. If the calculated Gd anomaly is higher than 1.1, it implies that there may be an extra discharge of Gd which do not originate from crustal rocks. Rivers covering densely populated and heavily industrialized areas usually show positive Gd anomalies due to anthropogenic inputs (Bau and Dulski, 1996). In this study, the Gd anomaly (Gd_N/Gd_N^*) was calculated using the following equation (Ogata and Terakado, 2006; Hissler et al., 2015):

$$Gd_N/Gd_N^* = 5Gd_N / (2Nd_N + 3Dy_N) \quad (2)$$

Owing to the coherent properties of REEs, the normalized value of natural Gd concentration can be calculated by interpolating elements near Gd in the periodic table. The normalized value was calculated with the following equation:

$$\text{Gd}_N^* = (2\text{Nd}_N + 3\text{Dy}_N) / 5 \quad (3)$$

The Gd anomaly values in this study ranged from 1.4 to 4.0 (average: 2.3 ± 0.6 , $n = 102$). These values conform well with an earlier study, which showed values from 1.6 to 3.9 with an average of 2.3 ± 0.8 in the San Francisco Bay (Hatje et al., 2016). The positive Gd anomaly in this study can be interpreted that the water contains the anthropogenic component as well as the Gd from natural sources (Lawrence, 2009).

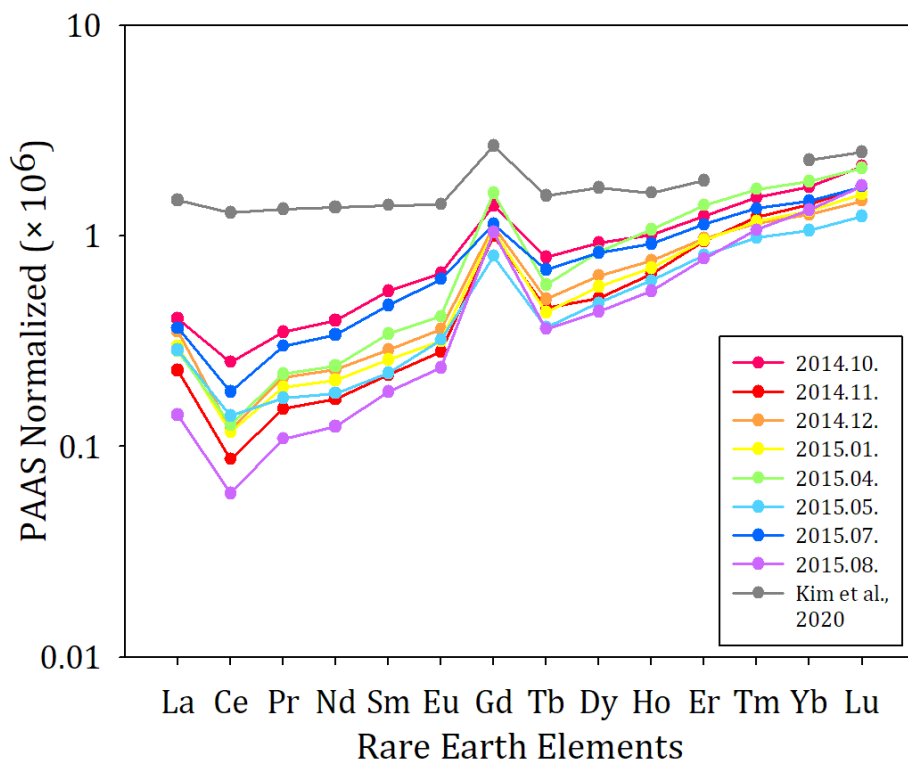


Figure 10. The monthly average PAAS (Post-Archean average Australian Shale) normalized patterns of dissolved REEs in the Nakdong River Estuary. The gray line indicates data collected in November 2017 from the same station (Kim et al., 2020).

3.2. Trace Metals

The distribution of dissolved trace metals against salinities is shown in Figure 11. The dissolved concentration of V, Mn, Fe, Co, Ni, Cu, Cd, and Mo each ranged from 10.89 to 38.15, 3.58 to 743.68, 4.57 to 230.23, 0.24 to 4.16, 14.45 to 78.27, 5.65 to 21.50, 0.06 to 0.41, and 6.74 to 96.28 nM, respectively (Table 6). Despite clean sampling, some of the samples were contaminated, and there were several outliers. The behavior of trace metals in the estuarine environment varies due to increased chemical gradients such as ionic strength, alkalinity, pH, and salinity (Church et al., 1986).

The features of dissolved trace metals-salinity distribution are described as follows.

(1) Distribution of dissolved Mn, Co, and Cd showed a generally positive correlation with increasing salinity. However, Mn and Co from October and July showed anomalously scattered distribution above the conservative mixing line in the low-salinity region. The trend was analogous to the LREEs. Also, the dissolved Mn concentration in May showed scattering in a higher salinity zone. Cd did not show any anomaly during the sampling period and showed a similar increasing trend with salinity with the concave curve upwards.

(2) Distribution of dissolved Ni was highly scattered in the low-salinity region, similar to Mn and Co. The highest concentration was approximately 4.5-folds greater than the lowest. The wide concentration ranges in low-salinity appeared to narrow down across salinity and eventually approached the oceanic endmember. The scatter in the low-salinity region indicates that the endmember in the estuary fluctuated during the sampling period.

(3) The concentration of dissolved Fe showed non-conservative behavior against increasing salinity. The concentrations were far below the conservative mixing line between the freshwater and seawater endmembers. There was an abrupt decrease in the low-salinity region, and the concentrations remained constant with increasing salinity.

(4) Conservative mixing was observed in dissolved Mo, V, and Cu. A negative correlation was shown in dissolved Cu, while Mo and V showed conservatively increasing trends with increasing salinity. The trends of the elements well indicated their source input; Cu originates from the river while Mo and V have their primary source in the ocean. Dissolved Mo showed conservative mixing throughout the whole sampling period, while the dissolved V concentration in July and August was placed above the conservative mixing line in the low to mid salinity region ($S = 0$ -12).

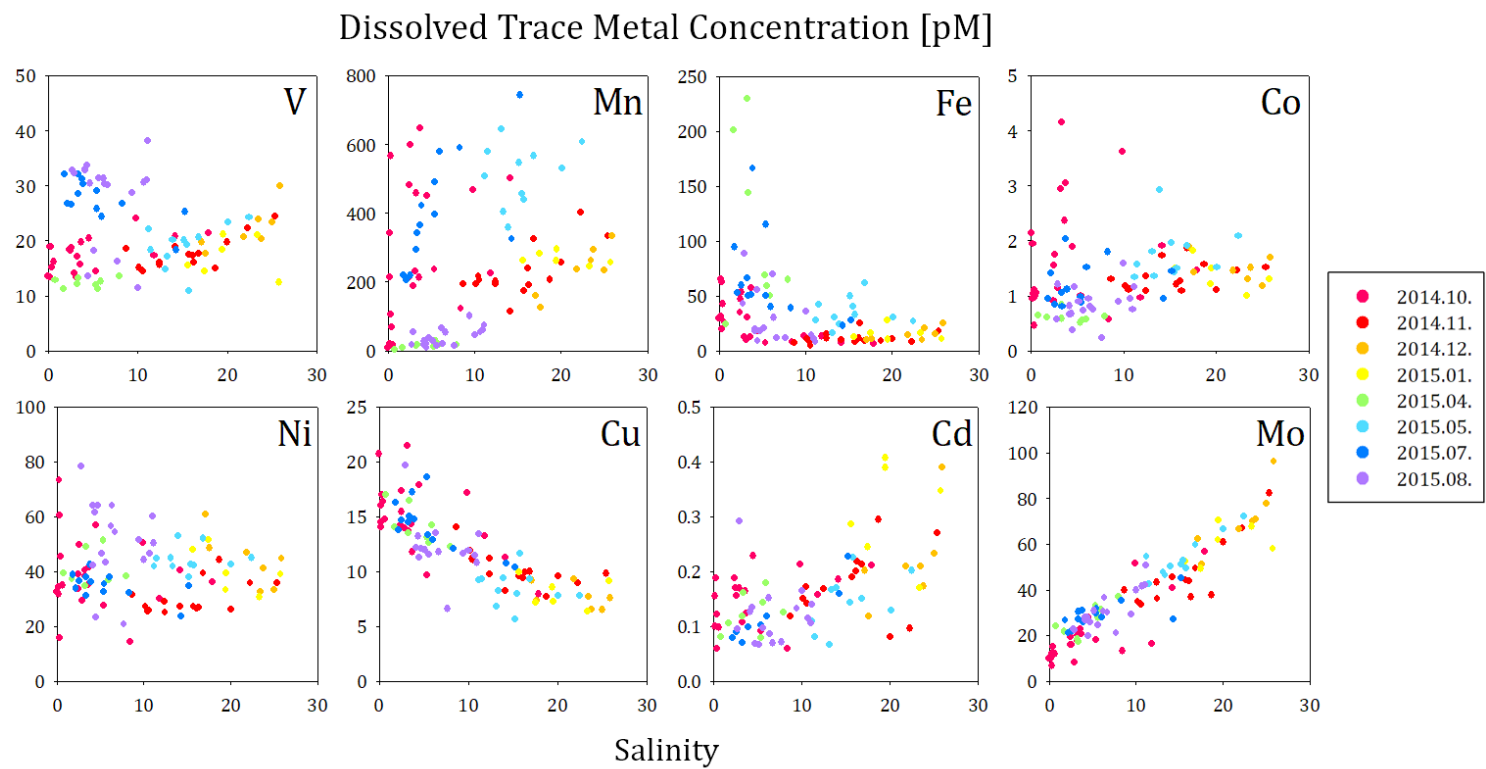


Figure 11. Dissolved concentrations of trace metals (V, Mn, Fe, Co, Ni, Cu, Cd, and Mo) against salinities in the Nakdong River Estuary.

Table 6. Concentrations of trace metals against salinities.

(N.D.: Not Detected, Numbers highlighted in red are considered as outliers.)

Sampling Time	Salinity	Concentrations of Trace Metals [nM]							
		V	Mn	Fe	Co	Ni	Cu	Cd	Mo
2014-10-23 15:00	0.2	18.9	342.7	65.7	1.04	73.3	16.0	0.19	11.2
2014-10-23 16:00	0.3	18.9	566.7	62.4	1.11	60.4	17.0	0.12	12.0
2014-10-23 17:00	0.4	15.2	68.7	42.6	0.99	45.6	16.4	0.06	15.1
2014-10-23 18:00	0.2	13.4	19.9	31.5	0.95	34.3	14.1	0.15	10.2
2014-10-23 19:00	0.2	13.6	8.0	30.0	2.15	32.5	20.7	0.54	9.8
2014-10-23 21:00	0.2	13.4	213.6	29.9	1.94	31.7	14.5	0.10	9.9
2014-10-23 22:00	0.6	16.2	15.9	26.1	1.06	34.9	14.8	0.10	11.9
2014-10-23 23:00	4.5	20.4	451.4	17.7	1.90	57.0	17.9	0.23	27.9
2014-10-24 1:00	2.5	18.8	599.1	53.4	1.75	49.8	17.4	0.16	16.1
2014-10-24 2:00	3.2	13.4	230.7	10.0	2.95	40.4	21.5	0.84	17.8
2014-10-24 3:00	3.7	19.7	647.2	57.6	3.05	41.5	11.8	0.12	20.7
2014-10-24 4:00	3.3	17.2	458.4	30.5	4.16	38.4	13.7	0.11	20.1
2014-10-24 5:00	2.5	18.3	482.9	47.2	1.56	39.1	15.4	0.17	15.9
2014-10-24 6:00	2.4	18.4	210.4	34.8	0.91	33.7	14.2	0.19	19.5
2014-10-24 7:00	2.9	14.1	188.1	12.4	1.14	29.4	14.0	0.17	8.1
2014-10-24 8:00	3.6	15.7	212.9	12.5	2.36	35.0	14.3	0.16	22.7
2014-10-24 10:00	9.9	24.1	469.1	13.7	3.62	50.5	17.2	0.21	51.8
2014-10-24 11:00	17.9	21.4	1118.4	6.6	1.46	36.1	7.9	0.21	56.9
2014-10-24 12:00	14.2	20.8	501.8	7.3	1.92	40.5	11.3	0.19	41.0
2014-10-24 13:00	11.8	17.4	224.7	13.2	0.96	30.1	13.3	0.16	16.4
2014-10-24 14:00	5.4	14.4	237.9	7.2	1.00	27.5	9.7	0.09	18.0
2014-10-24 15:00	3.1	N.D.	N.D.	N.D.	N.D.	N.D.	N.D.	N.D.	N.D.
2014-11-24 15:00	18.7	15.0	207.1	8.8	1.58	44.3	7.7	0.29	37.7
2014-11-24 17:00	16.8	17.6	325.4	9.2	1.86	39.6	10.0	0.21	49.3
2014-11-24 23:00	22.3	22.3	403.0	8.4	1.46	35.7	9.0	0.10	67.0
2014-11-25 1:00	15.7	17.5	175.0	8.2	1.21	27.1	9.6	0.19	44.3
2014-11-25 2:00	16.1	17.4	240.6	11.3	1.27	26.4	9.4	0.20	43.8
2014-11-25 3:00	14.2	18.9	114.2	9.7	1.73	27.4	8.2	N.D.	45.7
2014-11-25 4:00	12.4	16.1	193.3	11.2	1.35	29.0	9.8	N.D.	43.3
2014-11-25 5:00	10.6	14.4	204.8	4.6	1.10	25.7	11.0	0.14	33.7
2014-11-25 6:00	10.4	14.6	217.6	8.0	1.15	25.3	11.2	0.17	33.9
2014-11-25 7:00	8.7	18.5	193.3	7.4	1.31	31.4	14.0	0.12	39.8
2014-11-25 8:00	10.2	15.1	194.4	11.2	1.17	27.2	11.9	0.15	34.9
2014-11-25 9:00	12.4	15.6	201.4	15.7	1.09	25.2	11.2	0.17	36.2
2014-11-25 10:00	16.3	16.1	190.2	25.3	1.09	26.8	10.0	0.22	36.8
2014-11-25 12:00	25.4	24.5	335.1	17.7	1.52	35.9	9.8	0.27	82.3
2014-11-25 13:00	20.0	19.7	257.8	10.9	1.11	26.2	9.6	0.08	60.9
2014-12-22 17:00	17.6	17.6	126.5	10.7	1.42	48.6	7.3	0.12	51.3
2014-12-22 19:00	17.1	19.7	160.4	9.7	1.89	61.0	9.2	0.20	62.3
2014-12-22 23:00	21.8	20.7	237.2	14.3	1.46	47.0	9.3	0.21	66.7
2014-12-23 3:00	23.8	20.4	293.2	20.9	1.51	41.3	6.5	0.17	70.8
2014-12-23 5:00	25.9	29.9	334.8	25.1	1.70	44.7	7.6	0.39	96.3
2014-12-23 7:00	25.0	23.4	234.2	15.7	1.18	33.4	6.5	0.23	77.9
2014-12-23 13:00	23.5	23.9	261.7	10.3	1.30	32.5	7.7	0.21	69.9
2015-1-21 17:00	17.5	14.5	283.6	16.3	1.82	51.6	7.2	0.24	49.2
2015-1-21 19:00	15.6	15.5	262.5	12.9	1.50	47.9	9.9	0.29	52.5
2015-1-21 23:00	19.5	21.2	295.3	10.4	1.50	39.5	7.3	0.41	70.4
2015-1-22 3:00	25.7	12.4	256.9	10.9	1.30	39.0	9.2	0.35	57.9
2015-1-22 5:00	23.3	21.0	245.3	15.9	1.00	30.6	6.4	0.17	67.7
2015-1-22 7:00	19.4	18.4	261.0	27.8	1.22	33.3	8.6	0.39	61.8

Table 6. Concentrations of trace metals against salinities (Continued).
(N.D.: Not Detected, Numbers highlighted in red are considered as outliers.)

Sampling Time	Salinity	Concentrations of Trace Metals [nM]							
		V	Mn	Fe	Co	Ni	Cu	Cd	Mo
2015-4-21 11:00	5.3	12.0	10.4	69.0	0.51	51.4	13.1	0.08	32.9
2015-4-21 19:00	0.8	12.8	3.6	24.6	0.65	39.5	17.0	0.08	24.1
2015-4-21 21:00	1.7	11.3	8.7	201.6	0.61	37.3	14.0	0.11	21.7
2015-4-21 23:00	5.6	11.3	27.5	59.5	0.56	43.3	12.6	0.14	27.8
2015-4-22 3:00	7.9	13.6	18.1	65.0	0.62	38.3	12.3	0.13	37.0
2015-4-22 5:00	5.9	12.6	17.2	50.4	0.58	36.8	14.2	0.18	31.2
2015-4-22 7:00	3.3	12.2	15.6	230.2	0.58	34.6	13.5	0.12	18.3
2015-4-22 9:00	3.3	13.3	16.4	144.1	0.83	49.0	16.4	0.16	17.2
2015-5-19 17:00	13.9	20.1	358.1	24.5	2.93	52.9	9.4	0.17	50.3
2015-5-19 19:00	13.3	17.2	403.9	30.9	1.36	42.0	8.3	0.17	46.5
2015-5-19 21:00	15.5	19.2	457.0	40.7	1.42	42.7	8.0	0.14	52.7
2015-5-19 23:00	16.8	20.6	566.4	62.1	1.92	52.1	9.3	0.15	59.7
2015-5-20 1:00	15.8	10.9	440.4	32.7	1.49	42.3	11.6	0.23	49.5
2015-5-20 3:00	15.2	20.1	546.6	49.8	1.96	38.0	5.7	N.D.	51.2
2015-5-20 5:00	13.1	14.8	645.6	16.5	1.80	45.0	6.8	0.07	47.9
2015-5-20 7:00	11.5	18.3	578.6	42.4	1.57	44.9	9.3	0.08	42.4
2015-5-20 9:00	11.2	22.1	508.0	27.5	1.34	41.9	9.2	0.11	54.4
2015-5-20 11:00	20.1	23.4	531.8	30.5	1.52	42.6	7.8	0.13	66.5
2015-5-20 13:00	22.4	24.3	606.8	26.8	2.09	45.0	7.8	0.20	72.2
2015-7-15 12:00	6.0	24.3	579.4	40.0	1.52	38.0	12.9	0.12	28.2
2015-7-15 15:00	1.8	32.2	219.6	94.6	0.95	38.9	16.3	N.D.	26.8
2015-7-15 16:00	2.2	26.7	204.8	52.8	1.41	33.9	13.8	0.08	21.2
2015-7-15 17:00	2.5	26.6	218.5	59.7	0.85	36.6	14.7	0.09	21.8
2015-7-15 18:00	3.3	28.6	293.9	66.7	1.06	38.1	14.5	0.07	30.3
2015-7-15 19:00	3.8	31.3	365.7	51.3	2.04	42.4	17.2	N.D.	31.0
2015-7-15 20:00	5.4	25.8	395.8	50.6	0.88	35.5	13.3	N.D.	31.9
2015-7-15 22:00	15.2	25.3	743.7	27.8	1.45	34.7	10.4	0.23	45.1
2015-7-15 23:00	14.3	18.3	325.0	23.0	0.95	23.5	10.8	0.16	27.0
2015-7-16 0:00	8.3	26.8	590.9	39.0	1.79	32.2	12.1	N.D.	35.1
2015-7-16 1:00	5.4	29.1	489.9	115.1	0.97	32.5	18.6	0.10	29.8
2015-7-16 2:00	3.9	30.3	423.2	166.7	1.12	36.1	14.8	0.10	25.7
2015-7-16 3:00	3.4	32.1	343.1	50.2	0.81	31.0	15.0	N.D.	27.1
2015-8-26 12:00	2.9	32.3	54.5	88.8	1.21	234.3	19.7	0.29	22.3
2015-8-26 14:00	2.7	32.8	18.1	43.0	0.57	78.3	32.3	0.10	22.7
2015-8-26 16:00	4.1	32.8	27.6	19.9	0.81	64.1	62.7	0.13	26.7
2015-8-26 17:00	4.4	33.7	21.0	55.9	0.67	61.6	13.2	0.13	28.1
2015-8-26 18:00	4.7	30.4	37.7	17.7	1.16	64.0	12.1	0.07	25.8
2015-8-26 20:00	6.2	31.3	65.2	69.9	0.94	56.5	153.2	0.15	30.7
2015-8-26 21:00	11.0	31.1	61.1	11.0	0.75	60.1	10.8	0.11	42.1
2015-8-26 22:00	9.4	28.7	101.4	374.5	0.90	51.6	11.6	0.13	29.4
2015-8-26 23:00	6.7	30.1	53.2	11.7	0.74	54.4	11.8	0.07	30.1
2015-8-27 0:00	7.7	16.3	14.5	11.5	0.24	20.8	6.6	0.07	21.3
2015-8-27 1:00	5.1	18.2	29.5	20.6	0.90	46.5	11.9	0.07	30.8
2015-8-27 2:00	4.2	33.0	16.9	17.9	0.67	42.3	12.2	N.D.	27.9
2015-8-27 4:00	4.4	13.6	7.6	9.1	0.38	23.4	11.3	N.D.	20.0
2015-8-27 5:00	5.6	31.5	15.6	450.9	0.73	43.3	11.6	0.10	24.6
2015-8-27 6:00	6.3	30.3	19.8	30.2	0.81	64.2	13.5	0.09	36.7
2015-8-27 8:00	10.0	11.4	45.1	36.1	1.59	44.2	11.9	0.17	39.8
2015-8-27 9:00	10.7	30.6	55.0	14.7	0.95	46.5	11.4	0.12	41.5
2015-8-27 10:00	11.1	38.2	74.9	8.4	1.15	50.3	13.4	0.14	50.7

4. Discussion

4.1. Fractionation of the Dissolved Rare Earth Elements

The distribution of dissolved REEs with salinity showed generally conservative yet systematically changing trends (Figure 9). Such trends seem to depend on the river water endmember since the oceanic endmember conforms well with the earlier study conducted in the Nakdong River Estuary (Kim et al., 2020). The fractionation behavior of REEs appears to account for the varying trend along the series.

In the estuarine environment, REEs are rapidly removed from the dissolved phase in the low-salinity region by geochemical processes such as adsorption onto SPM and sediments and salt-induced riverine colloid coagulation (Sholkovitz, 1993; Kulaksız and Bau, 2007). Previous studies reported that removal of REEs occurring in the low-salinity region happens in order of LREE > MREE > HREE (Hoyle et al., 1984, Goldstein and Jacobsen, 1988, Elderfield et al., 1990, Sholkovitz et al., 1992, Sholkovitz, 1993, Sholkovitz, 1995, Nozaki et al., 2000b, Sholkovitz and Szymczak, 2000, Kulaksız, and Bau, 2007). LREEs being more particle reactive than HREEs leads to differing removal, which induces fractionation within the REE series. The extensive removal of LREEs results in a lower river water concentration, even lower than the seawater endmember. As the mixing of river water endmember and seawater with lower LREE concentration occurs, the distribution of LREEs may show a positive correlation with salinity. As the removal of REEs in river water decrease in systematic order across the series, heavier elements might not be removed as much as LREEs. The preferential removal of LREEs leads to a higher concentration of dissolved HREEs in river water than the seawater endmember. Therefore, the

fractionation behavior explains the negative correlation observed in heavier REE such as Yb and Lu.

The data in this study were compared with the previous study conducted at the Nakdong River Estuary in November 2017 in Figure 12 (Kim et al., 2020). The samples were collected by scooping along 13 stations, including the station where the collection was held in this study. The salinity of samples ranged from 0.3 to 33, and the elements La, Eu, and Lu are shown as representatives for each LREEs, MREEs, and HREEs. Under the assumption that the values gained in November 2017 well represent the surface distribution of the REEs, a trendline was made for each element with the given data, excluding samples that were collected near highly contaminated wastewater treatment plants. The dissolved REE concentration approaches the trendline as salinity increases, and this can be inferred that data from this study have similar seawater endmember with the sample of 2017. The graph showed that the data of La, Eu, and Lu collected in 2017 was up to 12, 7, 2-fold higher at the low-salinity region, respectively. This comparison may provide adequate evidence of fractionation behavior among the REE series, that the systematically varying extent of concentration across the series is likely to be the result of the fractionation of the REEs in the estuary.

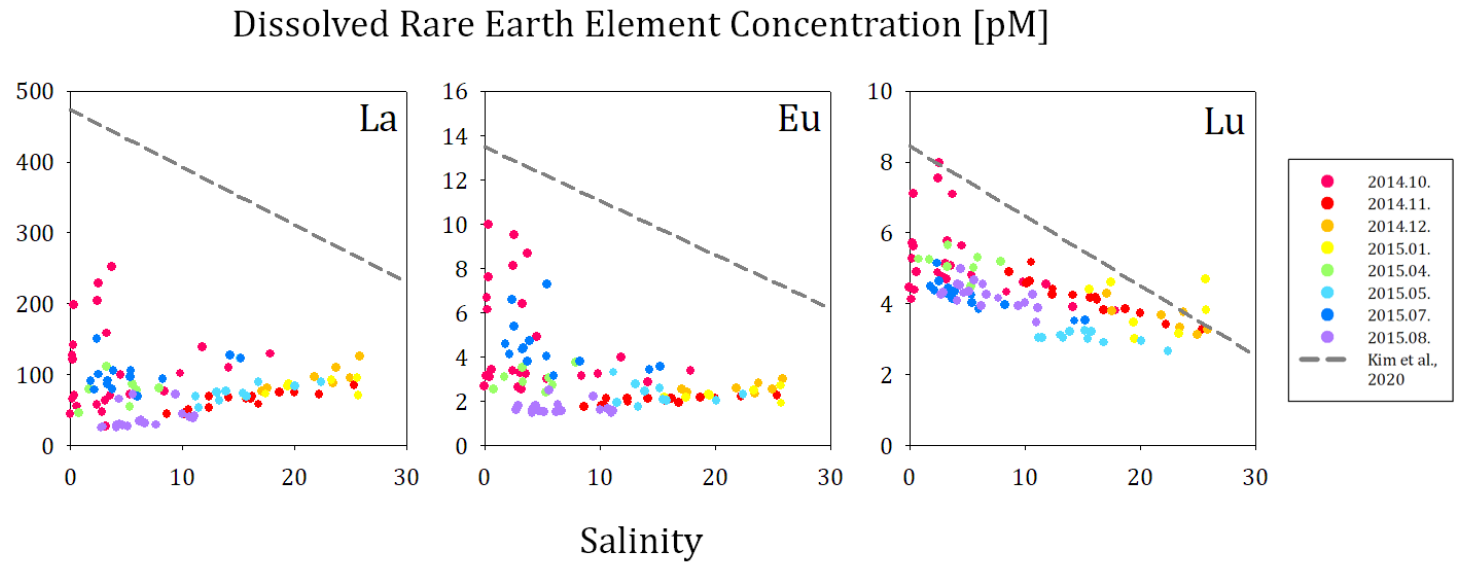


Figure 12. Graphs of dissolved La, Eu, Lu concentrations versus salinity in the Nakdong River Estuary. The trendline is made from the data collected in the Nakdong River Estuary, November 2017 (Kim et al., 2020).

4.2. Features Observed in Dissolved Rare Earth Elements and Trace Metals

The features of REE and trace metal profiles will be discussed to figure out the processes that govern the distribution of dissolved elements in the Nakdong River Estuary. The elements are classified into four groups: (1) Mn, Co, and LREEs, (2) Cd and Ni, (3) Fe, (4) Mo, V, Cu, and Gd.

4.2.1. Mn, Co, and LREEs

The profiles of dissolved Mn, Co, and LREEs showed a general increasing trend with exceptionally higher concentrations in October and July, which lies above the conservative mixing line in the low-salinity region. Cd showed an increasing trend with curved relation, which concaved upwards.

In Figure 9 and 11, Dissolved Mn, Co, and LREEs showed a wide range of concentrations above the conservative mixing line in the low-salinity region. The concentration of the two months reached the oceanic endmember with increasing salinity. LREE/HREE ratio was examined, and its correlation with salinity was plotted to figure out the process which may affect the overall increasing trend and two anomalous months (Figure 13). The ratio of LREE and HREE was utilized as an indicator for fractionation. The ratio was calculated with the following equation:

$$\text{LREE/HREE} = (\text{La}_N + \text{Pr}_N + \text{Nd}_N) / (\text{Er}_N + \text{Yb}_N + \text{Lu}_N) \quad (4)$$

The LREE/HREE ratio ranged from 0.07 to 0.32. When the value is below 1, this implies either depletion of LREEs or enrichment of HREEs from the crustal rock. The LREE/HREE-salinity plot showed a conservatively increasing trend with higher

values in October and July throughout the salinity region. Like the LREEs, the fractionation pattern of October and July was widely scattered in the low-salinity zone. The variant fractionation ratio in the two months near $S = 0$ suggests that the water discharged has already been fractionated inside the dam. The mechanism which is likely to cause fractionation and the scattered river water endmember is described below.

The redox reaction of dissolved Mn must be explained to understand the features of Mn, Co, and LREEs. The schematic diagram of dissolved Mn and other elements is depicted in Figure 14. Mn is a redox-sensitive element that usually exists in particulate form in aquatic conditions. The particle reactive Mn is rapidly removed from the river water through flocculation by vigorous mixing or precipitation by redox reactions (Morris and Bale, 1979; Klinkhammer and Bender, 1980; Sañudo-Wilhelmy et al., 1996; Audry, 2015). While dissolved Mn is precipitated as a form of Mn (hydr)oxides under oxic conditions, other dissolved elements such as particle reactive LREEs and Co are also adsorbed to the surface of oxides (Du Laing et al., 2009). During the precipitation, particulate Mn plays its role as a trace metal carrier as it carries the dissolved trace metals away to the sediments. When Mn (hydr)oxides reach the riverine sediments where oxygen is comparatively scarce, the oxides are reduced, releasing Mn back to the dissolved phase. Other trace metals adsorbed on the surface of oxides are also released in dissolved form during this process.

Through precipitation and redox reaction of Mn, the inhomogeneous vertical water columns of dissolved Mn, Co, and LREE are formed, and they are likely to result in various riverine endmember concentrations. The high volume of discharge also explains the scattered distribution in October and July in the low-salinity region. The average monthly discharge from the dam is shown in Table 7. October and July had a comparatively large amount of discharge compared to the other months. The

discharged river water in these months may contain not only the oxic surface waters with removed trace metals but also waters near suboxic benthic sediments, which may have a higher concentration of trace metals owing to desorption from Mn (hydr)oxide, as the floodgate of the dam is kept open to keep the water level steady.

The profile of the elements and the LREE/HREE ratio showed a positive correlation with increasing salinity in the mid to high-salinity region. Such trends imply that the discharged water, which has already been fractionated, does not go through significant changes. Concerning the scatter in the low-salinity region converging and approaching the saltwater endmember concentration with increasing salinity, the REE-salinity plot indicates that the physical mixing is the only mechanism that governs the concentration of REEs once the water is discharged (Figure 9).

Also, the discharge of suboxic water appears to account for the higher concentration of LREEs in April and Mn in May. The LREE/HREE ratio in April and May was higher than the mixing line. The distribution of both months suggests that the river water discharged in May and April may contain suboxic water near benthic sediments, containing regenerated trace metals and REEs.

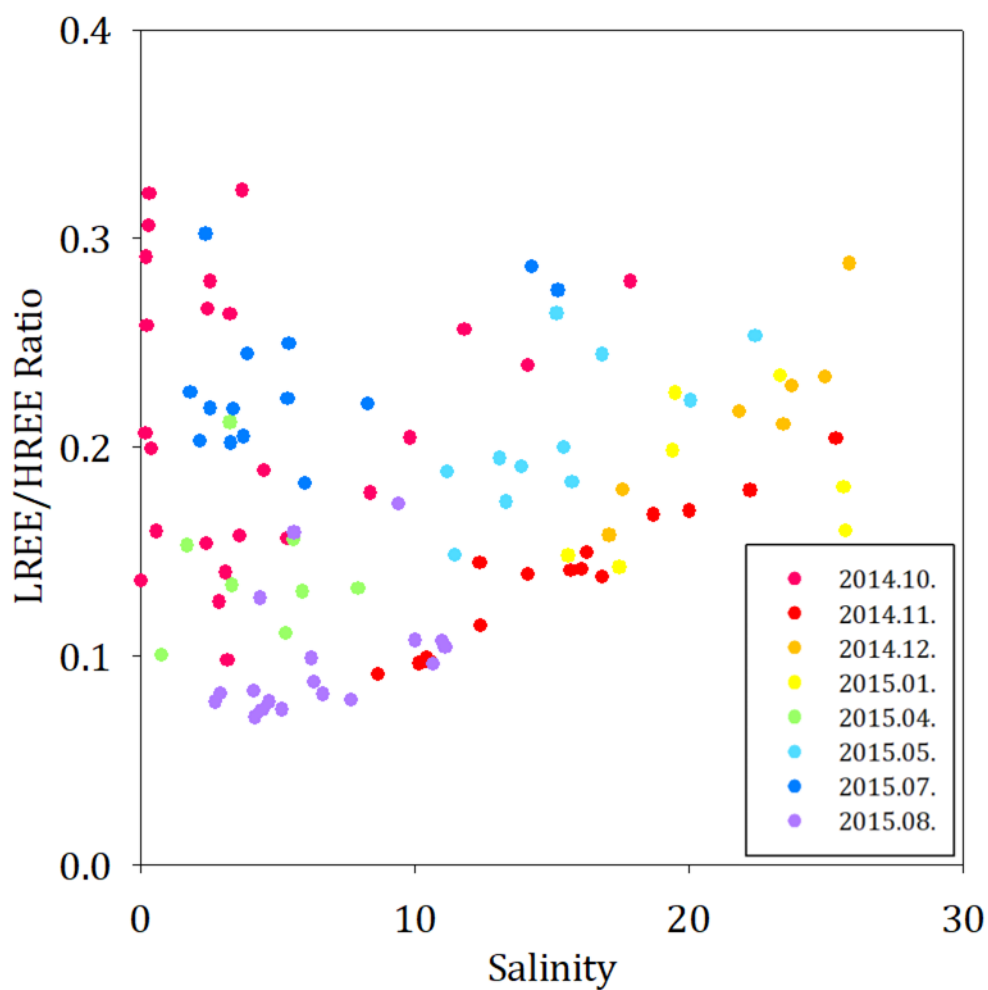


Figure 13. LREE/HREE ratio against salinities in the Nakdong River Estuary.

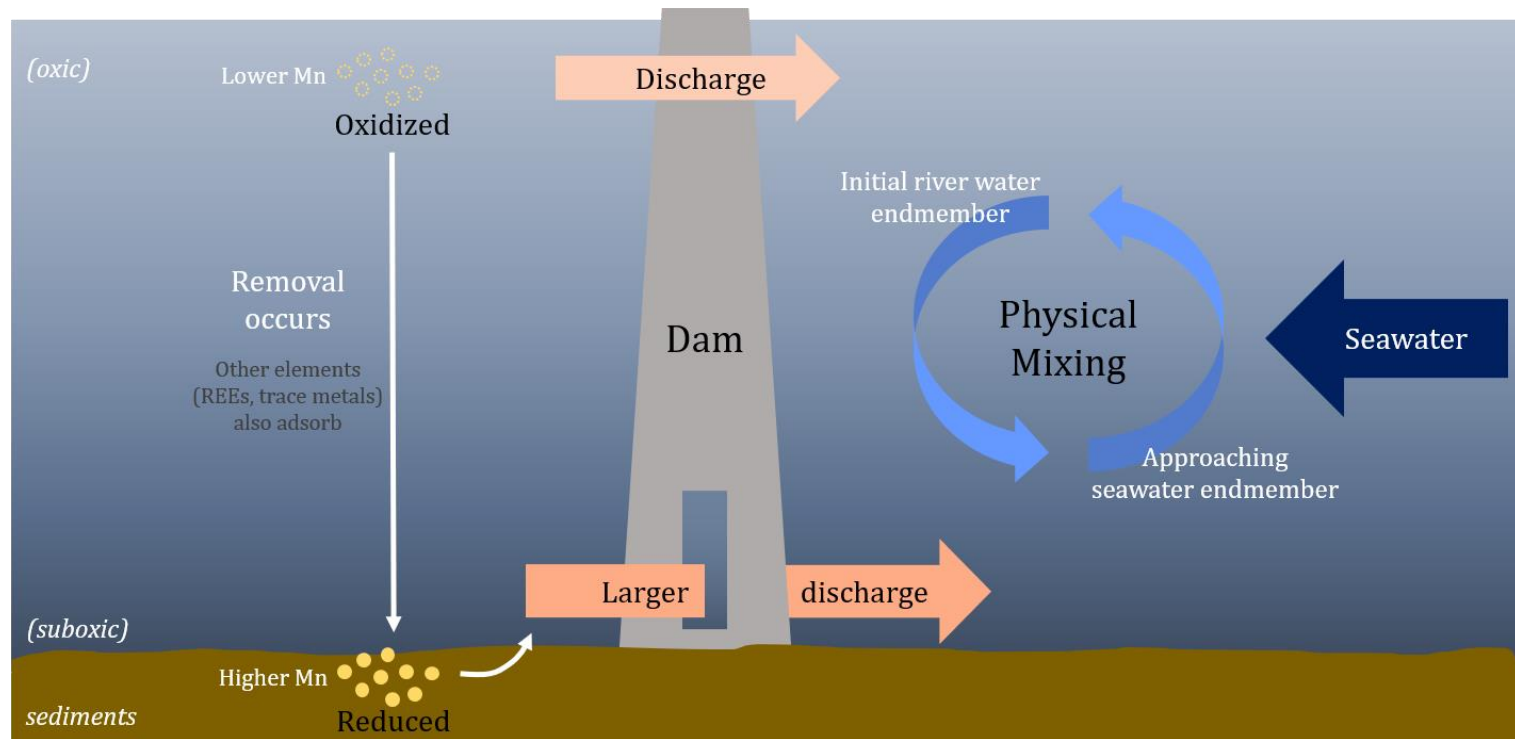


Figure 14. Conceptual diagram of redox reaction of Mn-oxide and function of the dam with respect to varying river water endmember concentration.

Table 7. The sample collection date, discharge, and average discharge value of the Nakdong River Estuary. The value of discharge is measured from the left bank drainage gate in the Nakdong River, where the sampling station is located.

Sampling Date	Discharge [m ³ /sec]	Average Discharge [m ³ /sec]	Sampling Date	Discharge [m ³ /sec]	Average Discharge [m ³ /sec]
2014-10-23	1313.798	925.495	2015-04-21	602.405	584.1025
2014-10-24	537.192		2015-04-22	565.8	
2014-11-24	77.686	214.769	2015-05-19	215.15	195.4605
2014-11-25	351.852		2015-05-20	175.771	
2014-12-22	57.38	57.0815	2015-07-15	658.648	597.9495
2014-12-23	56.783		2015-07-16	537.251	
2015-01-21	62.305	67.988	2015-08-26	457.66	385.0525
2015-01-22	73.671		2015-08-27	312.445	

4.2.2. Cd and Ni

The dissolved Cd and Ni profiles differed from the distribution of Mn, Co, and LREEs (Figure 11). Dissolved Ni showed scattered concentrations in the low-salinity region, which levels out and reaches the seawater endmember. The whole mechanism of the variant vertical distribution of oxic-suboxic water appears to explain the distribution of Ni, which also showed a wide range of concentrations in the low-salinity region. The decrease in the range of dissolved Ni concentration with increasing salinity and reaching the oceanic endmember reflects the physical mixing between freshwater and seawater. On the other hand, the dissolved Cd-salinity plot showed a positive correlation with a curve that concaved upwards. Previous studies reported that Cd shows such a trend and has the highest concentration in the high-salinity region by forming stable Cd-chloro complexes in the high-salinity region (Comans and van Dijk, 1988; Hatje et al., 2003; Wang and Liu, 2003). The behavior of Cd indicates that the element is more affected by the redox reaction after released from the dam.

4.2.3. Fe

In this study, the concentration of Fe had a range of 4.6 - 230.2 nM, and approximately 75% of them were below 50nM (Figure 11). The abrupt decrease of dissolved Fe observed in the low-salinity region can be explained by the rapid removal in an estuarine environment. Fe is a particle-reactive element that usually exists in particulate form rather than dissolved form once introduced in estuaries. Both field and experimental studies were conducted to determine the chemical speciation of dissolved Fe and the removal mechanism of dissolved Fe in estuaries. The drastic removal in the low-salinity region observed in earlier studies explains

the phenomenon with flocculation by turbulent mixing, precipitation of Fe oxide-organic matter colloids with seawater cations, and adsorption onto SPM and sediments (Boyle et al., 1977; Klinkhammer and Bender, 1981; Sharp et al., 1982; Byrd et al., 1990; Shiller and Boyle, 1991; Sañudo-Wilhelmy et al., 1996; Takanayagi and Gobeil, 2000; Wang and Liu, 2003). The feature observed in this study appears to be the result of removal by flocculation.

4.2.4. Mo, V, Cu, and Gd

The positive correlation of Mo and V with salinity results from conservative mixing between freshwater and oceanic endmember. Seawater is known as the primary source of both elements. Previous studies showed that Mo and V exist at $\sim 105 \text{ nmol kg}^{-1}$ and $30\text{-}36 \text{ nmol kg}^{-1}$ respectively in the form of oxyanion in seawater with long residence time, which indicates that the concentration of the elements is constant in the ocean (Collier, 1984; Sohrin et al., 1989; Bruland & Lohan, 2003). The seawater endmember in this study conforms well with the reported oceanic concentrations. The dissolved V concentration in July and August were higher than the conservative mixing line. Since the behavior of dissolved V in estuaries is not standardized, former studies suggest that V may show higher concentration by forming complexes with dissolved organic carbon (Emerson and Huested, 1991), the vast amount of river water discharge (Caccia and Millero, 2003), or the intrusion of oxygenated seawater (Wang and Sañudo-Wilhelmy, 2009). The mechanism which governs the V concentration in Nakdong River Estuary remains unclear.

Conservative negative correlations with increasing salinity were observed in dissolved Cu and Gd. Such trends can be interpreted as the result of stable complexation. Cu is known to have a higher river endmember since it originates from

riverine sources, including crustal rocks. The element shows strong complexation with organic ligands, which can stay stable in the dissolved phase. Conservative mixing happens in estuaries by diluting the stable organo-ligand complex as saltwater mixes with the river water (Boyle et al., 1982; Shiller and Boyle, 1991; Windom et al., 1996; Sañudo-Wilhelmy et al., 1996; Zwolsman et al., 1997). In this study, Cu showed a high correlation with humic dissolved organic matters and dissolved organic carbon (Figure 15).

Distinct from other MREEs, dissolved Gd showed a conservative mixing trend, similar to HREEs. Such a phenomenon seems to result from the additional input of dissolved Gd by anthropogenic activities (Kulaksız and Bau, 2007). The high stability of Gd released from human activities owes to their chelation with ligands such as Gd-DTPA and Gd-BT-DO3A to prevent adverse biological effect (Künnemeyer et al., 2009; Rogosnitzky and Branch, 2016; Hatje et al., 2018). The anthropogenic fraction of Gd is calculated in the following section.

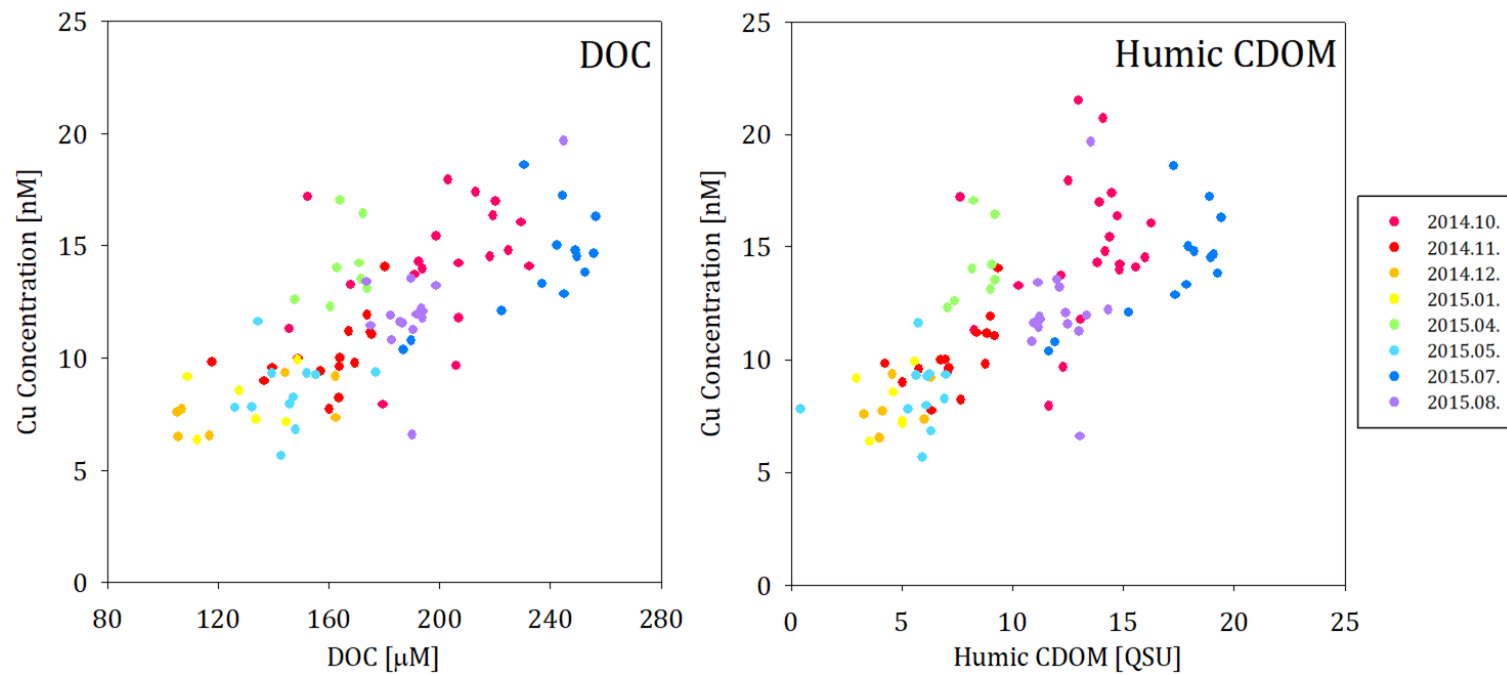


Figure 15. Dissolved Cu concentration against dissolved organic carbon and humic colored dissolved organic matter in the Nakdong River Estuary.

4.3. The Anthropogenic Fraction of Gd

Based on the assumption that the excess concentration of Gd stems only from human activities, the fraction of natural and anthropogenic Gd is examined. "Anthropogenic" and "Natural" Gd concentration which each of them has its origin from anthropogenic activities and natural sources, were estimated by utilizing the following equation (Figure 16):

$$[\text{Gd}_{\text{Anthropogenic}}] = [\text{Gd}] - [\text{Gd}_{\text{Natural}}] \quad (5)$$

$[\text{Gd}]$ is a term for measured dissolved Gd concentrations from the river. The interpolated value $[\text{Gd}_{\text{Natural}}]$ can be estimated as follows:

$$[\text{Gd}_{\text{Natural}}] = \text{Gd}_N^* \times [\text{Gd}_{\text{PAAS}}] \quad (6)$$

Where Gd_N^* is calculated by equation (3) and $[\text{Gd}_{\text{PAAS}}]$ is the Gd concentration of PAAS (Taylor and McLennan, 1985).

The monthly average concentrations and percentage of each $\text{Gd}_{\text{Natural}}$ and $\text{Gd}_{\text{Anthropogenic}}$ are calculated in Table 8. Figure 17 shows the average fraction of each source per month. The Gd had its lowest concentration in May (23.93 nM) and the highest in April (47.48 nM), and the anthropogenic input of Gd ranged from 39.7% (July) to 67.9% (August) of measured Gd concentration. Both the concentration of Gd and the fraction of Gd did not show a significant correlation with seasonal variation nor the discharge from the dam. The result supports that anthropogenic Gd is solely dependent on the amount of discharge by human activities, and it stays in a dissolved form as the element by chelation with ligands.

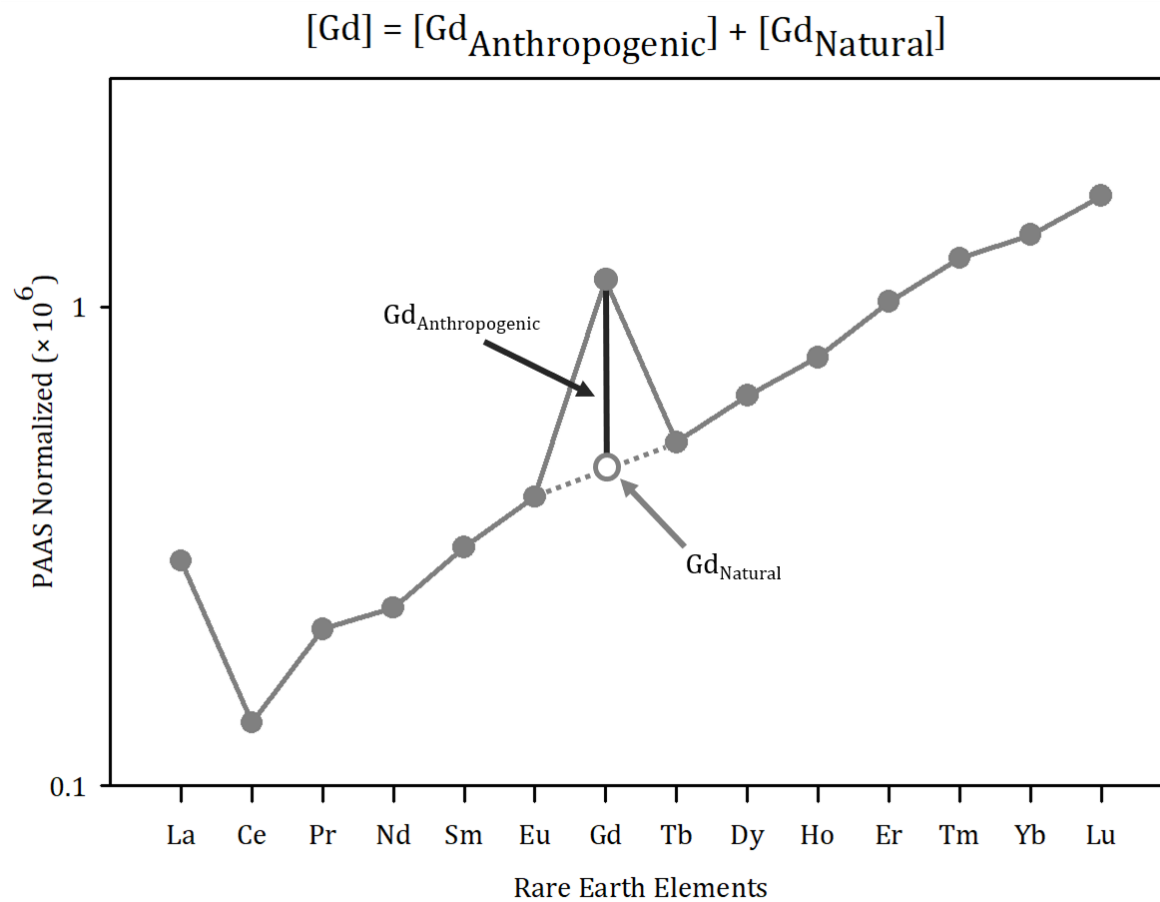


Figure 16. Schematic diagram of calculating anthropogenic and natural fraction in dissolved Gd.

Table 8. Calculated values of monthly average anthropogenic and natural Gd concentrations and their proportions.

Sampling Time	Gd [pM]	Gd _{Natural} [pM]	Gd _{Anthropogenic} [pM]	Gd _{Natural} [%]	Gd _{Anthropogenic} [%]
2014.10.	41.40	23.00	18.39	55.6	44.4
2014.11.	31.68	11.66	20.02	36.8	63.2
2014.12.	33.38	15.03	18.36	45.0	55.0
2015.01.	31.54	13.29	18.25	42.1	57.9
2015.04.	47.48	19.13	28.35	40.3	59.7
2015.05.	23.93	11.24	12.69	47.0	53.0
2015.07.	33.91	20.44	13.47	60.3	39.7
2015.08.	31.04	9.98	21.06	32.1	67.9

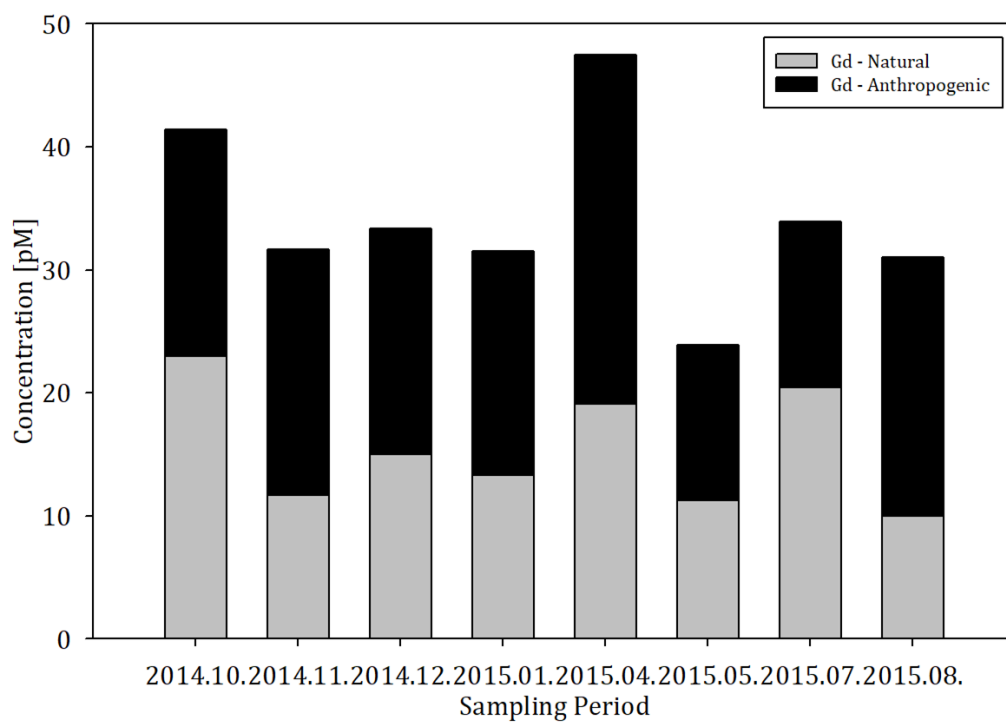


Figure 17. Calculated fractions of monthly average natural and anthropogenic Gd from the Nakdong River Estuary.

Conclusion

The concentrations of dissolved REEs and trace metals (V, Mn, Fe, Co, Ni, Cu, Cd, and Mo) were examined to investigate the process governing the distribution of elements and influence of a dam that regulates the freshwater discharge throughout the whole season in the Nakdong River Estuary, where sheds heavily urbanized cities in Korea.

The REEs presented systematically changing conservative mixing trends with two anomalous months (October and July). The varying distribution across the series seems to result from different endmember of the REEs in the low-salinity region by fractionation behavior. Particle-reactive LREEs appear to be more prone to the geochemical reaction, which may cause the lower river water endmember. PAAS-normalized values showed negative Ce anomaly by scavenging insoluble tetravalent Ce and positive Gd anomaly by anthropogenic input.

The profile of dissolved Mn, Co, and LREEs showed a general increasing trend against increasing salinity. October and July behaved anomalously with a wide range of freshwater endmember. The LREE/HREE ratio suggests the scattered concentration in the low-salinity region due to fractionation, which is likely to occur before the discharge. The redox reaction of dissolved Mn and ad/desorption of other elements onto Mn (hydr)oxide in surface water seems to govern the distribution of Mn, Co, and LREEs. The large discharge of the inhomogeneous vertical water column in October and July from the dam, including both oxic and suboxic water, seems to cause a wide range of riverine endmember. The physical mixing between each endmember accounts for the dissolved concentrations reaching the oceanic endmember in the mid to high-salinity region.

The profile of Ni can also be explained with the same mechanism with Mn and other elements, while Cd showed an increasing trend, which appears to be the result of complexation with chlorides in seawater. Fe showed an abrupt decrease in the low-salinity region, which suggests the drastic removal by flocculation. Since Mo and V originate from the ocean, they both showed a conservative increase, yet the process which accounts for high dissolved V concentration in July and August is still ambiguous. Cu and Gd both showed a stable negative correlation with increasing salinities owing to complexation behavior with organic ligands and chelation, respectively.

The fraction of natural and anthropogenic Gd was estimated by interpolating the adjacent values. The calculated value implies that the anthropogenic Gd depends solely on the input from the river, not released nor removed from the estuarine environment. The trend of natural Gd with increasing salinity showed similar behavior to other MREEs, but anthropogenic Gd remains dissolved in stable form by chelating with ligands.

This study displays the distribution of dissolved REEs and trace metals, the geochemical and physical mixing process that governs the behavior of elements, and the influence of the dam in estuarine waters downstream throughout the whole season. Further studies on riverine fluxes considering the regulated water flow might be necessary for a deeper understanding of the global circulation of elements.

Bibliography

- Audry, S., Blanc, G., Schäfer, J., Guérin, F., Masson, M., & Robert, S. (2007). Budgets of Mn, Cd and Cu in the macrotidal Gironde estuary (SW France). *Marine Chemistry*, 107(4), 433-448.
- Bau, M., & Dulski, P. (1996). Anthropogenic origin of positive gadolinium anomalies in river waters. *Earth and Planetary Science Letters*, 143(1-4), 245-255.
- Bau, M., Knappe, A., & Dulski, P. (2006). Anthropogenic gadolinium as a micropollutant in river waters in Pennsylvania and in Lake Erie, northeastern United States. *Geochemistry*, 66(2), 143-152.
- Bender, M. L., & Gagner, C. (1976). Dissolved copper, nickel and cadmium in the Sargasso Sea. *J. mar. Res.*, 34(3), 327-339.
- Boyle, E. A., Edmond, J. M., & Sholkovitz, E. R. (1977). The mechanism of iron removal in estuaries. *Geochimica et Cosmochimica Acta*, 41(9), 1313-1324.
- Boyle, E. A., Husted, S. S., & Grant, B. (1982). The chemical mass balance of the Amazon Plume—II. Copper, nickel, and cadmium. *Deep Sea Research Part A. Oceanographic Research Papers*, 29(11), 1355-1364.
- Boyle, E. A., Sclater, F., & Edmond, J. M. (1976). On the marine geochemistry of cadmium. *Nature*, 263(5572), 42-44.
- Boyle, E., & Edmond, J. M. (1975). Copper in surface waters south of New Zealand. *Nature*, 253(5487), 107-109.
- Brand, L. E., Sunda, W. G., & Guillard, R. R. (1983). Limitation of marine phytoplankton reproductive rates by zinc, manganese, and iron 1. *Limnology and oceanography*, 28(6), 1182-1198.

- Breuer, E., & Sañudo-Wilhelmy, S. A. (1999). Trace metals and dissolved organic carbon in an estuary with restricted river flow and a brown tide bloom. *Estuaries*, 22(3), 603-615.
- Bruland, K. W., & Lohan, M. C. (2003). Controls of Trace Metals in Seawater. *TrGeo*, 6, 625.
- Bruland, K. W., Franks, R. P., Knauer, G. A., & Martin, J. H. (1979). Sampling and analytical methods for the determination of copper, cadmium, zinc, and nickel at the nanogram per liter level in sea water. *Analytica chimica acta*, 105, 233-245.
- Byrd, J. T., Lee, K. W., Lee, D. S., Smith, R. G., & Windom, H. L. (1990). The behavior of trace metals in the Geum Estuary, Korea. *Estuaries*, 13(1), 8-13.
- Caccia, V. G., & Millero, F. J. (2003). The distribution and seasonal variation of dissolved trace metals in Florida Bay and adjacent waters. *Aquatic Geochemistry*, 9(2), 111-144.
- Chester, R. (2009). *Marine geochemistry*. John Wiley & Sons.
- Church, T. M., Tramontano, J. M., & Murray, S. (1986). Trace metal fluxes through the Delaware Bay estuary. *Rapports et Proces-Verbaux des Reunions-Conseil International pour L'Exploration de la Mer*, 186, 271-276.
- Collier, R. W. (1984). Particulate and dissolved vanadium in the North Pacific Ocean. *Nature*, 309(5967), 441-444.
- Comans, R. N., & van Dijk, C. P. (1988). Role of complexation processes in cadmium mobilization during estuarine mixing. *Nature*, 336(6195), 151-154.
- Cooper, L. H. N. (1935). Iron in the sea and in marine plankton. *Proceedings of the Royal Society of London. Series B-Biological Sciences*, 118(810), 419-438.

- De Baar, H. J., Bacon, M. P., Brewer, P. G., & Bruland, K. W. (1985). Rare earth elements in the Pacific and Atlantic Oceans. *Geochimica et Cosmochimica Acta*, 49(9), 1943-1959.
- Du Laing, G., Rinklebe, J., Vandecasteele, B., Meers, E., & Tack, F. M. (2009). Trace metal behaviour in estuarine and riverine floodplain soils and sediments: a review. *Science of the total environment*, 407(13), 3972-3985.
- Elbaz-Poulichet, F., Seidel, J. L., & Othoniel, C. (2002). Occurrence of an anthropogenic gadolinium anomaly in river and coastal waters of Southern France. *Water research*, 36(4), 1102-1105.
- Elderfield, H. (1988). The oceanic chemistry of the rare-earth elements. *Philosophical Transactions of the Royal Society of London. Series A, Mathematical and Physical Sciences*, 325(1583), 105-126.
- Elderfield, H., Upstill-Goddard, R., & Sholkovitz, E. R. (1990). The rare earth elements in rivers, estuaries, and coastal seas and their significance to the composition of ocean waters. *Geochimica et Cosmochimica Acta*, 54(4), 971-991.
- Emerson, S. R., & Husted, S. S. (1991). Ocean anoxia and the concentrations of molybdenum and vanadium in seawater. *Marine Chemistry*, 34(3-4), 177-196.
- Gaillardet, J., Viers, J., & Dupré, B. (2003). Trace elements in river waters. *TrGeo*, 5, 605.
- Goldberg, E. D., Koide, M., Schmitt, R. A., & Smith, R. H. (1963). Rare-Earth distributions in the marine environment. *Journal of Geophysical Research*, 68(14), 4209-4217.
- Goldstein, S. J., & Jacobsen, S. B. (1988). REE in the Great Whale River estuary, northwest Quebec. *Earth and Planetary Science Letters*, 88(3-4), 241-252.
- Harvey, H. (1960). *The Chemistry and Fertility of Sea Waters* / H. W. Harvey.

- Hatje, V., Apte, S. C., Hales, L. T., & Birch, G. F. (2003). Dissolved trace metal distributions in port jackson estuary (sydney harbour), Australia. *Marine Pollution Bulletin*, 46(6), 719-730.
- Hatje, V., Bruland, K. W., & Flegal, A. R. (2016). Increases in anthropogenic gadolinium anomalies and rare earth element concentrations in San Francisco Bay over a 20 year record. *Environmental science & technology*, 50(8), 4159-4168.
- Hatje, V., Lamborg, C. H., & Boyle, E. A. (2018). Trace-metal contaminants: human footprint on the ocean. *Elements*, 14(6), 403-408.
- Hissler, C., Hostache, R., Iffly, J. F., Pfister, L., & Stille, P. (2015). Anthropogenic rare earth element fluxes into floodplains: Coupling between geochemical monitoring and hydrodynamic sediment transport modelling. *Comptes Rendus Geoscience*, 347(5-6), 294-303.
- Holzbecher, E., Knappe, A., & Pekdeger, A. (2005). Identification of degradation characteristics—exemplified by Gd–DTPA in a large experimental column. *Environmental Modeling & Assessment*, 10(1), 1-8.
- Hoyle, J., Elderfield, H., Gledhill, A., & Greaves, M. (1984). The behaviour of the rare earth elements during mixing of river and sea waters. *Geochimica et Cosmochimica Acta*, 48(1), 143-149.
- ICOLD (2020). ICOLD world register of dams, computer database. International Committion on Large Dams, Paris. <https://www.icold-cigb.org/>
- Jakubowski, N., Moens, L., & Vanhaecke, F. (1998). Sector field mass spectrometers in ICP-MS. *Spectrochimica Acta Part B: Atomic Spectroscopy*, 53(13), 1739-1763.
- Jeong, K. S., Kim, D. K., & Joo, G. J. (2007). Delayed influence of dam storage and discharge on the determination of seasonal proliferations of *Microcystis*

- aeruginosa and *Stephanodiscus hantzschii* in a regulated river system of the lower Nakdong River (South Korea). *Water Research*, 41(6), 1269-1279.
- Johannesson, K. H., Stetzenbach, K. J., & Hodge, V. F. (1997). Rare earth elements as geochemical tracers of regional groundwater mixing. *Geochimica et Cosmochimica Acta*, 61(17), 3605-3618.
- Kim, T., Kim, H., & Kim, G. (2020). Tracing river water versus wastewater sources of trace elements using rare earth elements in the Nakdong River estuarine waters. *Marine Pollution Bulletin*, 160, 111589.
- Klinkhammer, G. P., & Bender, M. L. (1981). Trace metal distributions in the Hudson River estuary. *Estuarine, Coastal and Shelf Science*, 12(6), 629-643.
- Klinkhammer, G., Elderfield, H., & Hudson, A. (1983). Rare earth elements in seawater near hydrothermal vents. *Nature*, 305(5931), 185-188.
- Knappe, A., Möller, P., Dulski, P., & Pekdeger, A. (2005). Positive gadolinium anomaly in surface water and ground water of the urban area Berlin, Germany. *Geochemistry*, 65(2), 167-189.
- Kulaksız, S., & Bau, M. (2007). Contrasting behaviour of anthropogenic gadolinium and natural rare earth elements in estuaries and the gadolinium input into the North Sea. *Earth and Planetary Science Letters*, 260(1-2), 361-371.
- Kulaksız, S., & Bau, M. (2011). Rare earth elements in the Rhine River, Germany: first case of anthropogenic lanthanum as a dissolved microcontaminant in the hydrosphere. *Environment International*, 37(5), 973-979.
- Kulaksız, S., & Bau, M. (2013). Anthropogenic dissolved and colloid/nanoparticle-bound samarium, lanthanum and gadolinium in the Rhine River and the impending destruction of the natural rare earth element distribution in rivers. *Earth and Planetary Science Letters*, 362, 43-50.

- Künnemeyer, J., Terborg, L., Nowak, S., Brauckmann, C., Telgmann, L., Albert, A., ... & Karst, U. (2009). Quantification and excretion kinetics of a magnetic resonance imaging contrast agent by capillary electrophoresis-mass spectrometry. *Electrophoresis*, 30(10), 1766-1773.
- Lawrence, M. G., Ort, C., & Keller, J. (2009). Detection of anthropogenic gadolinium in treated wastewater in South East Queensland, Australia. *Water research*, 43(14), 3534-3540.
- Lee, S. A., & Kim, G. (2018). Sources, fluxes, and behaviors of fluorescent dissolved organic matter (FDOM) in the Nakdong River Estuary, Korea. *Biogeosciences*, 15(4).
- Libes, S. (2011). *Introduction to marine biogeochemistry*. Academic Press.
- Ma, L., Dang, D. H., Wang, W., Evans, R. D., & Wang, W. X. (2019). Rare earth elements in the Pearl River Delta of China: Potential impacts of the REE industry on water, suspended particles and oysters. *Environmental Pollution*, 244, 190-201.
- Migaszewski, Z. M., & Gałuszka, A. (2015). The characteristics, occurrence, and geochemical behavior of rare earth elements in the environment: a review. *Critical reviews in environmental science and technology*, 45(5), 429-471.
- Millward, G. E. (1995). Processes affecting trace element speciation in estuaries. A review. *Analyst*, 120(3), 609-614.
- Moeller, P., Dulski, P., Bau, M., Knappe, A., Pekdeger, A., & Sommer-von Jarmersted, C. (2000). Anthropogenic gadolinium as a conservative tracer in hydrology. *Journal of Geochemical Exploration*, 69, 409-414.
- Morel, F. M., & Price, N. M. (2003). The biogeochemical cycles of trace metals in the oceans. *Science*, 300(5621), 944-947.

- Morris, A. W., & Bale, A. J. (1979). Effect of rapid precipitation of dissolved Mn in river water on estuarine Mn distributions. *Nature*, 279(5711), 318-319.
- Nozaki, Y., Lerche, D., Alibo, D. S., & Tsutsumi, M. (2000a). Dissolved indium and rare earth elements in three Japanese rivers and Tokyo Bay: evidence for anthropogenic Gd and In. *Geochimica et Cosmochimica Acta*, 64(23), 3975-3982.
- Nozaki, Y., Lerche, D., Alibo, D. S., & Snidvongs, A. (2000b). The estuarine geochemistry of rare earth elements and indium in the Chao Phraya River, Thailand. *Geochimica et Cosmochimica Acta*, 64(23), 3983-3994.
- Ogata, T., & Terakado, Y. (2006). Rare earth element abundances in some seawaters and related river waters from the Osaka Bay area, Japan: significance of anthropogenic Gd. *Geochemical Journal*, 40(5), 463-474.
- Pavoni, E., Crosera, M., Petranich, E., Oliveri, P., Klun, K., Faganeli, J., ... & Adami, G. (2020). Trace elements in the estuarine systems of the Gulf of Trieste (northern Adriatic Sea): A chemometric approach to depict partitioning and behaviour of particulate, colloidal and truly dissolved fractions. *Chemosphere*, 126517.
- Piepgras, D. J., & Jacobsen, S. B. (1992). The behavior of rare earth elements in seawater: Precise determination of variations in the North Pacific water column. *Geochimica et Cosmochimica Acta*, 56(5), 1851-1862.
- Rapp, I., Schlosser, C., Rusiecka, D., Gledhill, M., & Achterberg, E. P. (2017). Automated preconcentration of Fe, Zn, Cu, Ni, Cd, Pb, Co, and Mn in seawater with analysis using high-resolution sector field inductively-coupled plasma mass spectrometry. *Analytica chimica acta*, 976, 1-13.
- Rogosnitzky, M., & Branch, S. (2016). Gadolinium-based contrast agent toxicity: a review of known and proposed mechanisms. *Biometals*, 29(3), 365-376.

- Rogowska, J., Olkowska, E., Ratajczyk, W., & Wolska, L. (2018). Gadolinium as a new emerging contaminant of aquatic environments. *Environmental toxicology and chemistry*, 37(6), 1523-1534.
- Sañudo-Wilhelmy, S. A., & Flegal, A. R. (1996). Trace metal concentrations in the surf zone and in coastal waters off Baja California, Mexico. *Environmental science & technology*, 30(5), 1575-1580.
- Sharp, J. H., Culbertson, C. H., & Church, T. M. (1982). The chemistry of the Delaware estuary. General considerations 1. *Limnology and Oceanography*, 27(6), 1015-1028.
- Sherry, A. D., Caravan, P., & Lenkinski, R. E. (2009). Primer on gadolinium chemistry. *Journal of Magnetic Resonance Imaging: An Official Journal of the International Society for Magnetic Resonance in Medicine*, 30(6), 1240-1248.
- Shields, G., & Stille, P. (2001). Diagenetic constraints on the use of cerium anomalies as palaeoseawater redox proxies: an isotopic and REE study of Cambrian phosphorites. *Chemical Geology*, 175(1-2), 29-48.
- Shiller, A. M. (2002). Seasonality of dissolved rare earth elements in the lower Mississippi River. *Geochemistry, Geophysics, Geosystems*, 3(11), 1-14.
- Shiller, A. M., & Boyle, E. A. (1991). Trace elements in the Mississippi River Delta outflow region: behavior at high discharge. *Geochimica et Cosmochimica Acta*, 55(11), 3241-3251.
- Sholkovitz, E. R. (1993). The geochemistry of rare earth elements in the Amazon River estuary. *Geochimica et Cosmochimica Acta*, 57(10), 2181-2190.
- Sholkovitz, E. R. (1995). The aquatic chemistry of rare earth elements in rivers and estuaries. *Aquatic geochemistry*, 1(1), 1-34.

- Sholkovitz, E. R., & Copland, D. (1981). The coagulation, solubility and adsorption properties of Fe, Mn, Cu, Ni, Cd, Co and humic acids in a river water. *Geochimica et Cosmochimica Acta*, 45(2), 181-189.
- Sholkovitz, E. R., & Schneider, D. L. (1991). Cerium redox cycles and rare earth elements in the Sargasso Sea. *Geochimica et Cosmochimica Acta*, 55(10), 2737-2743.
- Sholkovitz, E. R., Shaw, T. J., & Schneider, D. L. (1992). The geochemistry of rare earth elements in the seasonally anoxic water column and porewaters of Chesapeake Bay. *Geochimica et Cosmochimica Acta*, 56(9), 3389-3402.
- Sholkovitz, E., & Szymczak, R. (2000). The estuarine chemistry of rare earth elements: comparison of the Amazon, Fly, Sepik and the Gulf of Papua systems. *Earth and Planetary Science Letters*, 179(2), 299-309.
- Sohrin, Y., Isshiki, K., Nakayama, E., Kihara, S., & Matsui, M. (1989). Simultaneous determination of tungsten and molybdenum in sea water by catalytic current polarography after preconcentration on a resin column. *Analytica chimica acta*, 218, 25-35.
- Sohrin, Y., Urushihara, S., Nakatsuka, S., Kono, T., Higo, E., Minami, T., ... & Umetani, S. (2008). Multielemental determination of GEOTRACES key trace metals in seawater by ICPMS after preconcentration using an ethylenediaminetriacetic acid chelating resin. *Analytical Chemistry*, 80(16), 6267-6273.
- Tagliabue, A., Bowie, A. R., Boyd, P. W., Buck, K. N., Johnson, K. S., & Saito, M. A. (2017). The integral role of iron in ocean biogeochemistry. *Nature*, 543(7643), 51-59.
- Takayanagi, K., & Gobeil, C. (2000). Dissolved aluminum in the upper St. Lawrence Estuary. *Journal of oceanography*, 56(5), 517-525.

- Taylor, S. R., & McLennan, S. M. (1985). The continental crust: its composition and evolution.
- Wang, D., & Wilhelmy, S. A. S. (2009). Vanadium speciation and cycling in coastal waters. *Marine Chemistry*, 117(1-4), 52-58.
- Wang, Z. L., & Liu, C. Q. (2003). Distribution and partition behavior of heavy metals between dissolved and acid-soluble fractions along a salinity gradient in the Changjiang Estuary, eastern China. *Chemical Geology*, 202(3-4), 383-396.
- Windom, H., Byrd, J., Smith Jr, R., Hungspreugs, M., Dharmvanij, S., Thumtrakul, W., & Yeats, P. (1991). Trace metal-nutrient relationships in estuaries. *Marine Chemistry*, 32(2-4), 177-194.
- Yeghicheyan, D., Carignan, J., Valladon, M., Le Coz, M. B., Cornec, F. L., Castrec-Rouelle, M., ... & Dia, A. (2001). A compilation of silicon and thirty one trace elements measured in the natural river water reference material SLRS-4 (NRC-CNRC). *Geostandards newsletter*, 25(2-3), 465-474.
- Zhang, J., & Nozaki, Y. (1996). Rare earth elements and yttrium in seawater: ICP-MS determinations in the East Caroline, Coral Sea, and South Fiji basins of the western South Pacific Ocean. *Geochimica et Cosmochimica Acta*, 60(23), 4631-4644.
- Zhao, Q., Liu, S., Deng, L., Yang, Z., Dong, S., Wang, C., & Zhang, Z. (2012). Spatio-temporal variation of heavy metals in fresh water after dam construction: a case study of the Manwan Reservoir, Lancang River. *Environmental monitoring and assessment*, 184(7), 4253-4266.
- Zwolsman, J. J., Van Eck, B. T., & Van Der Weijden, C. H. (1997). Geochemistry of dissolved trace metals (cadmium, copper, zinc) in the Scheldt estuary, southwestern Netherlands: impact of seasonal variability. *Geochimica et Cosmochimica Acta*, 61(8), 1635-1652.

요약문 (국문 초록)

전 세계의 70%가 넘는 강의 방류가 댐으로 조절되고 있지만, 희토류 원소와 미량금속의 강에서 해양으로의 유입과정에서의 댐의 역할에 대한 연구는 아직 많이 진행되지 못하였다. 하구에서의 혼합 과정과 댐의 역할을 알아보기 위하여, 전 계절에 걸쳐 채취한 낙동강 강물 시료의 용존 희토류와 미량금속을 분석하였다. 측정 전 미량으로 존재하는 분석 원소들을 농축하기 위하여 해수자동분석기(seaFAST)를 이용하였으며, 유도결합 플라즈마 질량 분석기(HR-ICP-MS)로 시료 중 희토류원소와 미량금속의 농도를 측정하였다. 염분과 낙동강 하구에서 희토류원소의 상관관계에서 원소들은 유사하게 보존적으로 혼합된 양상을 띠었으나, 담수 단성분의 점진적인 감소로 인하여 기울기의 변화를 보였다. 이는 분별작용으로 인해 일어난 현상으로 보인다. 표준지질물질(PAAS)로 정규화시킨 희토류원소의 경우 채수 시점의 모든 시료들이 가벼운 희토류원소(LREE)가 무거운 희토류원소(HREE)에 비해 농도가 낮았다는 점으로 미루어보아 분별작용이 일어났음을 확인할 수 있었다. 미량금속의 경우 Mn 과 Co 는 염도가 증가함에 따라 농도가 늘어났지만 2014 년 10 월과 2015 년 7 월의 경우 저염분대에서 분산된 경향의 높은 농도를 보였으며, 이는 LREE 와 유사했다. 해당 현상은 강물에서 Mn 의 산화/환원 과정에서 다른 원소들이 흡/탈착됨에 따라 불균일한 농도로 존재하게 되는 수괴가 그대로 댐을 통해 방출됨에 따라 관찰된 것으로 보인다. 저염분대에서 보이던 분산의 경우 담수와 해수의 물리적 혼합을 통해

염도가 높아질 수록 그 분산도가 낮아지며 해수 쪽 단성분에 수렴하는 것을 확인할 수 있었다. Mn의 산화/환원 작용은 Ni의 분포에도 영향을 미쳤으며, 이와 다르게 Cd의 경우 해수 속 염화물과 강한 결합을 보였다. Fe는 전계절에 걸쳐 저염분대에서 응집에 의해 다량으로 제거가 일어났다. Mo와 V는 해수를 기원으로 하는 원소들로 염도의 증가에 따라 보존적으로 증가하였고, Cu와 Gd는 각각 용존유기탄소, 킬레이트와의 안정적인 화합물 형성으로 염도가 증가할수록 농도가 희석되어 감소하였다. 측정한 희토류원소의 값을 통해 인류 발생의 Gd와 자연계에 존재하는 Gd의 분율을 계산하여 본 결과 인류 기원의 Gd는 댐에서의 방출 이후로 계속 안정성을 띄고 있음을 확인하였다. 본 연구 결과는 낙동강 하구에서의 용존 희토류원소와 미량금속의 분석을 통해 하구에서 일어나는 화학적, 물리적 반응을 분석하였으며 댐 내부에서 일어나는 반응이 강물 기원 플릭스에 영향을 미칠 수 있음을 시사한다.

주요어: 하구; 희토류원소; 미량금속; 산화환원반응; 담수-해수 혼합; 댐

학번: 2019-23097